Aalto University
School of Chemical
Engineering

Matthew Smyth

COLLOIDAL LIGNIN PARTICLES FOR WEATHERING PROTECTION IN WOOD COATINGS

Master´s Programme in Chemical, Biochemical and Materials Engineering
Major in Fibre and Polymer Engineering

Master's thesis for the degree of Master of Science in Technology
submitted for inspection, Espoo, 10 August, 2017.

Supervisor	Professor Monika Österberg
Instructor	Ph.D. Timo Leskinen

Author Matthew Smyth

Title of thesis Colloidal Lignin Particles for Weathering Protection in Wood Coatings

Degree Programme Chemical, Biochemical and Materials Engineering

Major Fibre and Polymer Engineering

Thesis supervisor Professor Monika Österberg

Thesis advisor(s) / Thesis examiner(s) Dr. Timo Leskinen

Date August 10, 2017 **Number of pages** 49 **Language** English

Abstract

Earth's changing climate and the better understanding of harmful impacts caused by humans has increased the demand for more sustainable products. Lignin is a material that offers renewability, is safe for humans and the environment and is already a by-product of industry. This work uses a recently developed technique for preparing colloidal lignin particles (CLPs) and deploying them into water based industrial wood stain as a UV protectant. The initially transparent stains with added CLPs took on the dark brown color of lignin, with concentration of CLPs having only minor effect. The dispersions remained stable after CLP addition however, viscosity was drastically decreased with a strong correlation with CLP concentration. Siberian larch and spruce wood were coated with the standard commercial stains and stains with 1:1, 1:1.5, and 1:2 ratios of commercial UV absorber to CLP concentrations. Coated wood samples were then exposed to simulated sunlight for 92 hours. Changes in color and UV reflectance spectra were recorded, as well as periodic photographs during exposure. The CLP coated samples go through a more drastic magnitude of color change compared to uncoated (NAT) and standard (STD) samples, however the change in relation to initial color is much less. Additionally, the color after 92 hours of exposure is much closer to the initial color in CLP samples due to an almost cyclical change. Reflectance spectroscopy revealed further differences between CLP samples and both the STD and NAT samples. CLP samples showed a large decrease in absorption in the UVA region but little change in the UVB region. NAT samples showed a similar decrease in the UVA region but with a shifted peak, but also had strong decreases in absorption in the UVB region. The STD samples experienced a more uniform decrease in absorption, with some regions having higher and others lower changes in absorption compared to CLP samples. The overall effectiveness of CLPs remains somewhat uncertain due to the inability to remove the coatings from the wood beneath and see the color. This work did reveal however, some positive outcomes that indicate CLPs could be used effectively in industrial wood coatings. There were strong differences in the color and absorption changes between CLP samples and the NAT and STD samples. This indicates that the CLPs were changing instead of the wood beneath. Although the extent of protection is still uncertain, it can be concluded here that CLPs have potential for use as UV protectants in wood coatings.

Keywords lignin, wood coatings, colloidal particles

Table of Contents

Table of Figures

1 Introduction

Scientific discovery has enabled the development of vast and rapidly changing technologies that have changed the way we see and interact with the world around us. Our society has become increasingly aware of the impact we are having on the environment and our health, which has led to demand for higher emphasis on sustainable development. Sustainable development encompasses a large number of topics but one major one is the reduction of dependence on energy-intensive and non-renewable materials. Bio-based alternatives are being studied and engineered to be replace metals and petroleum products in applications where they can compete practically and economically. Wood is a renewable material with numerous applications and will continue to be one of our most valuable resources. In many applications however, wood suffers from a drawback that, like many biomaterials is also one of its biggest benefits. The natural degradation of wood is something that is desirable in the scope of a circular economy, however undesirable until the wood has fulfilled its use. In order to prevent premature degradation, wood is often impregnated or coated with weather resistant materials.

While wood is often used for its engineering properties, it also has great aesthetic appeal. For this reason, many coatings are made to be semi-transparent. In such coatings however, light, a pivotal contributor to the degradation of wood, is allowed to pass through the coating. Transparent UV-absorbing materials such as zinc oxide (ZnO) and titanium dioxide (TiO_2) nanoparticles are often used in these coatings to prevent this. As these materials have been discovered to have eco-toxic effects however, there is a need for more sustainable alternatives.[1-5] Lignin, one of the major components of biomass, has UV absorbing capabilities and has recently been prepared as colloidal nanoparticles in aqueous media.[6] This thesis work will explore the capabilities of these lignin particles as UV-absorbers in a commercial wood stain and their impacts on other weathering resistant properties.

2 Background

2.1 Wood

2.1.1 Wood as a Resource

Wood has been an essential material for humankind for centuries, used in tools, structures, decorations, vehicles and more. The renewable sourcing of wood, its aesthetic appeal, and its sound mechanical properties have kept it a competitive material even in the age of engineered materials. With a trend of sustainable development on the rise, it is likely that wood use may even increase in the coming decades. Wood is a natural material that has the inherent ability to decompose after death so that the organic material can return to the earth where the nutrients are then salvaged for new life. While this is a desirable trait in a natural ecosystem, it is not something that is desirable when wood is used for applications such as construction, decoration, or tools.

One important aspect of wood that is important to always consider is the variability in its properties. As a natural material, wood properties vary not only between different species and classes (softwood/hardwood) but also within these categories.[7-9] These properties can be affected by natural and uncontrollable occurrences such as growth rate of the tree, or by the processing techniques used to extract and refine the material. One significant different between species of wood is the specific gravity or density, which has implications on the material properties. Heavy woods tend to swell more from water absorption than do less dense species. This makes heavier woods more susceptible to warping and cracking due to swelling and shrinking stresses.[7] Juvinile or compression wood can have similar impacts. Juvinile wood is formed during the beginning of a tree's life, and the fibres in the cell are oriented differently than in normal wood. This causes difference in swelling strain and will cause stress gradients between the juvenile and normal wood.[7,8] Compression wood is formed when wood is forced to bend, causing the growth to continue in an asymmetrical way. This causes both swelling/shrinking related stress gradients as well as a weak strength compared to normal wood of the same density.[7]

The texture of wood cells also has impacts on the use of wood material, including how it degrades outdoors. The texture refers to the shapes and dimensions of the cells, which tend to be long and narrow in softwood and short with large diameter variation in hardwood.[7] Hardwood fibres are narrow like softwood, however hardwood contains more vessels, which are essentially pores in the wood. These pores can act as nucleation sites for erosion.[7]

2.1.2 Wood Weathering

The weathering of wood refers to the degradation of the material specifically from stresses caused by the weather. This does not include decay due to organisms such as fungi and insects, which results in different form of degradation (rot).[7] Weathering of a material is a result of a complex combination of factors, many of which have synergistic effects. These factors include moisture, sunlight, temperature, chemicals and wind.[7,10,11] Weathering is not unique to wood, and occurs to some extent for all materials, even mountains. Weathering is a result of surface changes in the material, both physical and chemical. For wood, the primary initiator and propagator of weathering is UV radiation from the sun.[7,10-13] The UV light is absorbed by organic material at the surface and degradation through photo-oxidation occurs. Weathering affects only the surface of the material and begins at first contact with sunlight. The first change is in color, followed by physical separation and deterioration of the surface fibres.[7,10,14] Even though changes in color can be seen even after a couple weeks of unprotected exposure, it can take more than a century to erode the wood surface by just 5 mm.[7] Upon prolonged UV exposure, wood that was previously smooth will develop rough surface artifacts such as checks and cracks.

UV radiation that is absorbed by wood causes chemical changes in the wood components, which results in color changes. These color changes have been described as an initial yellowing or browning, followed by development into grey.[10,11,14] These chemical changes occur only within the surface layer of the wood, up to 2.5 mm.[10] The primary component responsible for the color changes is lignin, which absorbs a broad spectrum of UV light. Extractives found in varying quantities in wood can also absorb light in the visible region of the electromagnetic spectrum.[7,15,16] Cellulose and hemi-cellulose can contribute as well, absorbing strongly below wavelengths of 200 nm. Studies have shown however, that surface wood that has become grey in color due to weathering consists almost of pure cellulose.[10] This is shown in Table 1 from the

Table 1 *Composition of wood from different species on the outer, middle and inner layers after outdoor exposure of 30 year adapted from Browne and Simonson (1957)*[17]

Species	**Cellulose**			**Lignin**		
	Inner	**Middle**	**Outer**	**Inner**	**Middle**	**Outer**
Western Red Cedar	48	48	44	42	28	7
Douglas Fir	50	46	47	36	30	7
Southern Pine	51	52	51	50	21	4
Yellow Poplar	51	59	62	27	15	2
Birch	55	57	60	28	21	6

work of Browne.[17] Overall, it is important to note that the species of wood has a very significant impact in both the nature and magnitude of color change when exposed to UV and visible light.[9,18]

While temperature itself does not weather the wood, it has an effect in combination with UV exposure. Absorption of UV or visible light results in a photo-oxidation reaction which, is accelerated as the temperature rises.[10] Even though UV radiation constitutes only a small fraction of the total irradiance hitting the surface of the Earth, it has a higher energy per photon. Energy of light decreases with increasing wavelengths as per Plank's law

$$E = hc/\lambda$$

where *E* is energy, *h* is Plank's constant, *c* is the speed of light and λ is the wavelength of light. The energies of UV photons are sufficient to break chemical bonds, which results in both radical formation and de-polymerization at the wood surface.[7] The spectrum of light hitting the Earth's surface is typically in the range of 295 – 3000 nm. In Table 2 some bond dissociation energies that apply to compounds found in wood, mostly lignin are shown. It can be seen that several of these bonds can be broken (forming free radicals) if sunlight is absorbed.

Table 2 *Bond dissociation energies of bonds found in wood matter and the corresponding wavelength of light required for dissociation adapted from Rånby and Rabek (1975)19*

Bond	**Bond Dissociation Energy (Kcal/mol)**	**Wavelength (nm)**
C–C (Aromatic)	124	231
C–H (Aromatic)	103	278
C–H (Methane)	102	280
O–H (Methanol)	100	286
C–O (Ethanol)	92	311
C–O (Methanol)	89	321
CH3COO–C (Methyl ester)	86	333
C–C (Ethane)	84	340
C–COCH3 (Acetone)	79	362
C–O (Methyl ether)	76	376

Moisture can also have impact wood weathering significantly, albeit by a different mechanism and effect compared with UV degradation. While light causes primarily chemical changes, water absorption creates physical stresses on wood.[10] When water is absorbed at the surface, it penetrates into the cell walls and causes the wood to swell. This creates a stress gradient between the surface and the bulk of the wood which then with sufficient magnitude and/or repetition results in physical deformation or damage.[10]

2.1.3 Wood Finishing

Wood finishing is necessary for several reasons. First, it keeps the wood (that is very porous) from collecting dirt and contaminates that may present a health hazard and degrade the wood. Another reason is to adjust the aesthetic properties of the wood, changing color, texture and or sheen.[20] The primary purpose of outdoor wood coatings or finishes is usually to protect the wood properties from weathering effects and preserve the esthetic quality. Many factors can affect how effective the coating is in these regards. Firstly, the wood itself has a major impact. Moisture content, density, texture, defects such as knots, chemical composition at the surface and growth ring size and orientation.[10,11] Also impacting the effects of weathering are of course the weather itself in that particular region, as well as other physical barriers present such as an overhanging roof shading the siding of a house. Lastly, the contents of the coating and how it is applied will impact how effective it is.

Wood finishes come in several varieties including but not limited to oils, lacquers, shellacs and varnishes. Wood stains use a combination of a binder (oil, varnish, lacquer, water-based) and colorant (pigment or dye) along with several other additives. The purpose of the binder is to hold

all the additional particles in place and create adhesion to the wood surface.[20] Stains can vary in their degree of penetration into the wood, with some forming only a film on top of the wood surface and others being absorbed by the wood cells. Finishes can be categorized in many ways based on their composition.[7] One of the most common is by the medium in which the functional components are suspended. Finishes can be oil, solvent, or water based with each having some benefit over the others.[7] Water-based coatings have become more popular recently in an effort and desire to phase out harmful VOC emissions from organic solvents.

For blocking UV absorption by the wood, pigmented coatings such as stains and paints are most effective.[11] There is often however, a desire to preserve the natural colors of the wood, for which there are also semi-transparent stains available. A water-borne, semi-transparent polymer stain forms a coating on the surface of the wood, which acts as a barrier to water penetration and physical weathering from wind and other abrasive contact. The drawback of semi-transparent finishes is their weak blocking of UV and short wavelength visible light from reaching the wood surface. Currently, the popular choice for this fix are inorganic nanoparticles such as zinc oxide, titanium oxide and cerium oxide.[4,11] While these materials are effective absorbers and appear transparent in a coating film, they have been demonstrated to have harmful effects on health and the environment.[1,2,5] For this reason, industry is searching for alternative UV absorbers that are more sustainable. Lignin is the natural UV absorbent in wood and is produced in vast quantity by the pulp and paper industry. It meets sustainability criteria, however its function as UV absorbent in wood coatings has not been directly demonstrated.

2.2 Lignin

2.2.1 Origin & Structure

Lignin is one of the three main components of lignocellulosic biomass, which additionally includes carbohydrates and extractives in several varieties and combinations. Lignin is an amorphous and highly branched biopolymer and is second only to cellulose in abundance within the category of natural polymers. When lignin is referred to as it is in plants, its native state, it is called protolignin. In wood, protolignin makes up about 18-35% of the dry mass and has both heterogeneous structure as well as distribution within the wood structure.[21,22] The biosynthesis

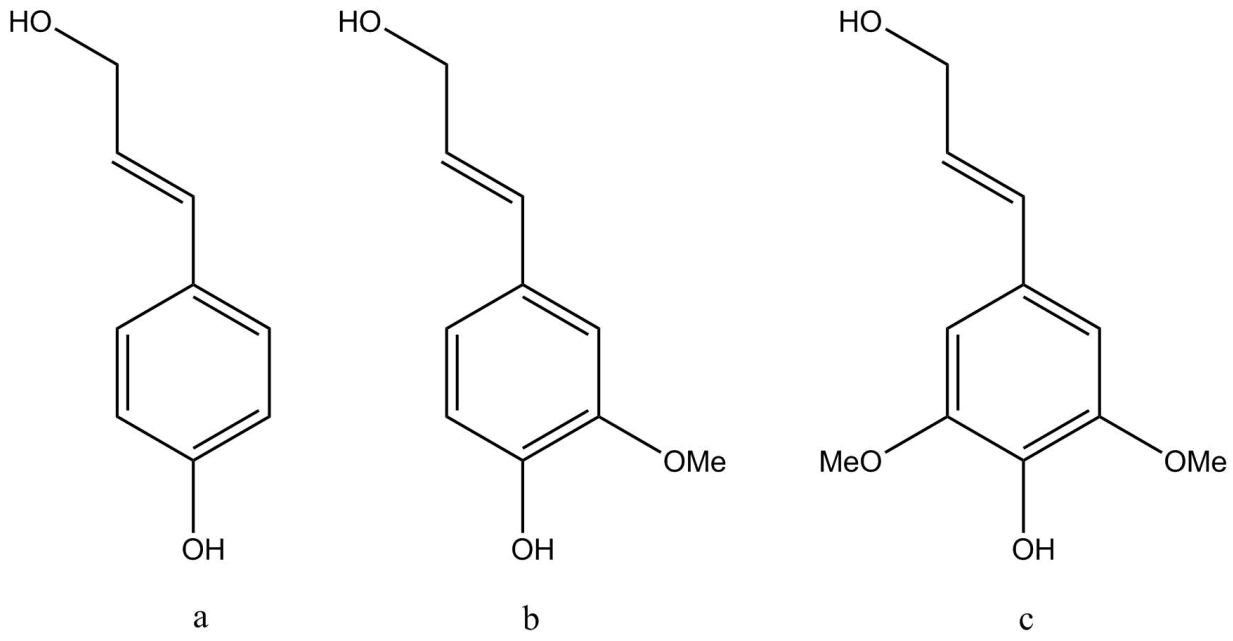

Figure 1 *Chemical structure of monolignols; p-coumaryl alcohol (a) coniferyl alcohol (b) and sinapyl alcohol (c)*

of lignin uses three precursor molecules with varying abundance and combinations that polymerize into a three-dimensional polymer bound together with C-O-C and C-C linkages. This combination is randomized to the extent that structure of lignin can vary greatly between species or even slightly between individual trees.[21]

These three pre-cursors, also known as monolignols are p-coumaryl alcohol, coniferyl alcohol and sinapyl alcohol. They are nearly identical (Figure 1) but have many possible bonding combinations, which results in the heterogeneous and somewhat random structure of lignin.[21] Within the lignin structure, these monolignols are referred to based on their unique bonding sites. Bonding to these sites are referred to as types p-hydroxyphenyl (p-coumaryl alcohol), guaiacyl (coniferyl alcohol) and syringyl (sinapyl alcohol). The biosynthesis of lignin begins with the oxidation of the phenolic hydroxyl groups on the pre-cursor molecules (monolignols). This is an enzymatically catalyzed electron transfer reaction resulting in free radical formation.[22] Delocalization of this free radical then yields many different bonding points for combining two radicalized precursor molecules (Figure 2).

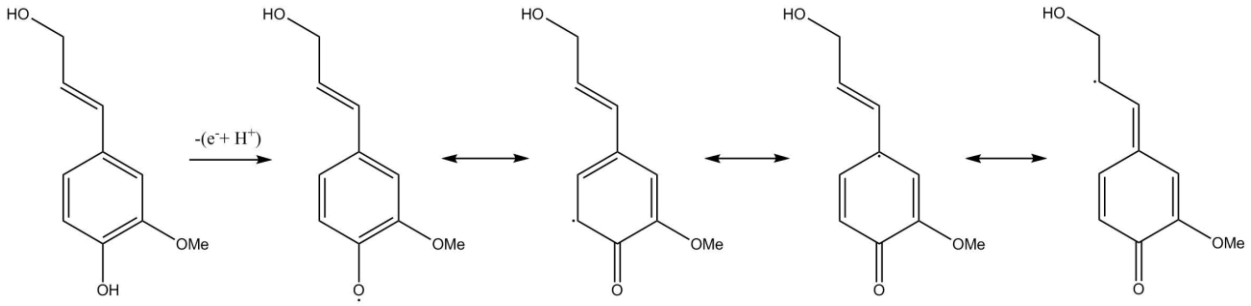

Figure 2 *Radicalization and mesomeric structures for coniferyl alcohol leading to multiple bonding (radical combination) possibilities*

The structure of protolignin remains a mystery due to molecular alterations during extraction, however the common linkages and their abundances in extracted lignin have been well documented (Table 3).[22] Carbon-carbon bonding makes up about a third of connecting linkages while ether bonds make up the remaining two thirds. The β-O-4 is the most common, making up 50-60% of the total linkages in wood biomass.[23] When this bond is broken during extraction, a reactive phenolic hydroxyl group is left, which contributes strongly to lignin reactivity and properties. Other functional groups are methoxyl groups and some aldehyde groups.[23] The properties of any given batch of extracted lignin depend not only on the inherent structure, which varies between species, but also strongly on the methods of extraction and isolation of the lignin from biomass.[24-26] Different extraction processes will yield different abundances of methoxyl, phenolic hydroxyl, aliphatic hydroxyl and carbonyl groups. Additionally, different processes may introduce functional groups to the lignin such as thiol groups in Kraft lignin.[27,28] For this work, Kraft lignin was used and thus will be the focus of discussion.

Table 3 *Relative abundance of different lignin bonds connecting the phenyl propane-units adapted from Chakar and Ragauskas (2014)*[22]

Linkage Type	**Dimer Structure**	**Approximate Abundance (%)**
β-*O*-4	Phenylpropane β-aryl ether	45 – 50
α-*O*-4	Phenylpropane α-aryl ether	6 – 8
β-5	Phenylcoumaran	9 – 12
5-5	Biphenyl and dibenzodioxocin	18 – 25
4-*O*-5	Diaryl ether	4 – 8
β-1	1,2-Diaryl propane	7 – 10
β-β	β-β-Linked structures	3

2.2.2 Properties

2.2.2.1 In Vivo

Although the exact structure of protolignin is not known, its properties and purpose within a living tree are. Protolignin is hydrophobic and facilitates the transport of water up the length of a tree.[25,29] While it is not the primary source of mechanical strength, it acts as a sort of glue that holds the cells together, acting as the soft, flexible matrix phase of the hierarchal composite that is wood.[25] Lignin also has antifungal and antimicrobial properties that protect wood from biological attack.[29] The fact that lignin is bio-based, biodegradable, and abundant amplifies the benefit for seeking industrial application. While these properties of protolignin are very desirable for many applications, manipulating this complex and heterogenous polymer after extraction and purification while maintaining natural properties remains a significant barrier to industrial use.[25,30,31]

2.2.2.2 Molecular Weight

Molecular weight variance of lignin arises from random cross linking during the radical polymerization and different degrees of degradation during extraction and purification processes.[25,32,33] Polydispersity of lignins is high, and materials typically contain constituents from oligomeric chains to highly polymerized structures.[34] These variations in lignin's physical and chemical structures make the species, as well as the extraction and purification methods important when sourcing as raw material. Even when analyzing these specific fractions of lignin, there has been some speculation that molecular weight analysis has not been accurate.[34] Since molecular weight plays an important role in the properties of lignin, this is an important area of research in order to achieve high value industrial lignin.

2.2.2.3 Solubility

The solubility of lignin is a very important factor especially in considering industrial application. Lignin is more hydrophobic than cellulose and hemicellulose; however, there are enough hydroxyl groups to allow hydrogen bonding to take place.[35] While Kraft lignin is mostly insoluble in water at neutral pH (some fractions are soluble), it has been shown that water increases the molecular mobility of lignin, which indicates a disruption of intermolecular hydrogen bonding.[36]

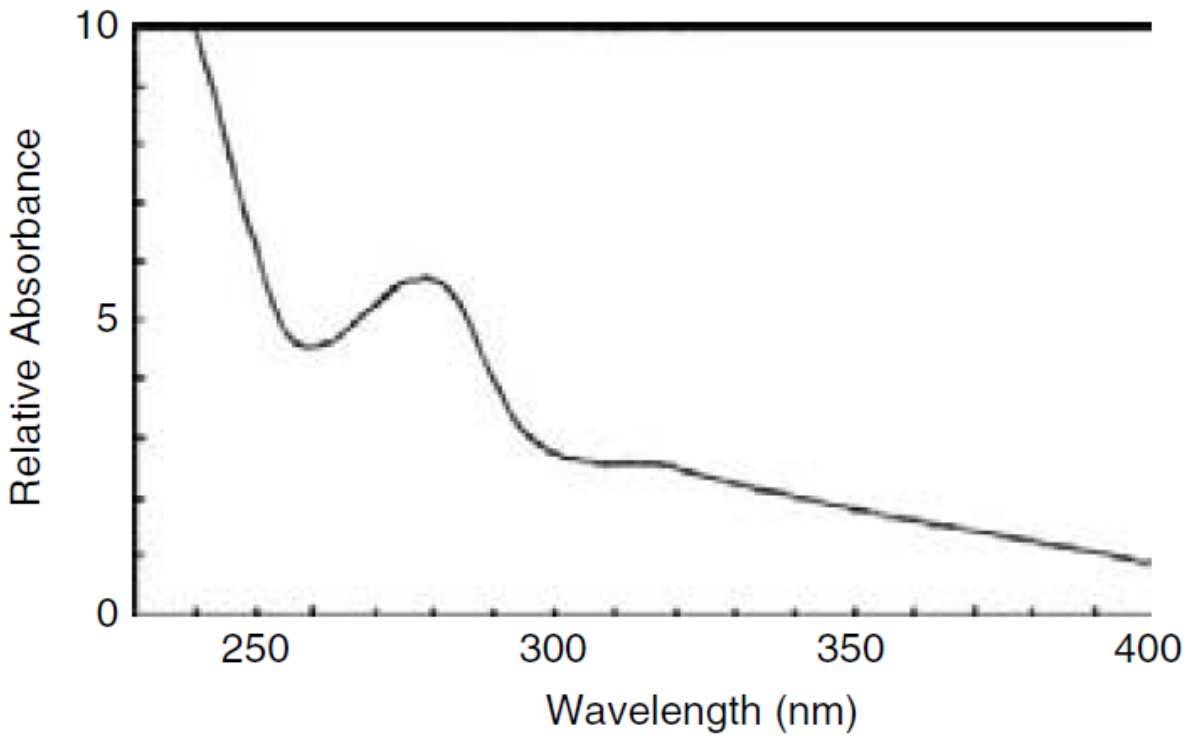

Figure 3 *UV absorption of lignin adapted from Williams (2012)*[7]

It is no surprise then that the addition of water to a lignin solution improves the solubility. The molecular weight can also impact solubility, and Kraft lignin tends to have a large distribution (0.6-180 kDa).[37] Different fractions of both the functionality and molecular mass make complete dissolution of Kraft lignin a difficult task.

2.2.2.4 Light Absorption

As mentioned earlier, lignin has several bonds that are susceptible to dissociation when light is absorbed. The UV absorption spectra for lignin is shown in Figure 3 from Williams (2012).[7] It can be seen here that there is a sharp absorption peak at 280 nm and a sharp increase below 260 nm which is common for many materials. Lignin's absorption of light can result in a number of reactions including bond cleavage and hydrogen abstraction. When the photon is absorbed, it can result in the formation of a free radical, which in the presence of oxygen and water can then form a hydroperoxide.[7] These reactions involving radical and peroxide formation will propagate in several chain reaction pathways which then leads to degradation of the polymer structure into

chromophoric components.[14,16] It is these chromophoric products of degradation that result in the changing color of lignin and wood after prolonged UV exposure.

The UV absorption spectra of lignin has been compared to colloidal lignin as well.[38-42] Li et al (2016) demonstrated a difference in absorption between Kraft lignin in solution and Kraft lignin nanospheres which were formed in similar fashion to this work.[39] The results showed the same characteristic absorption peak near to 280 nm but a broader shoulder of absorption into the visible region was present in the nanosphere spectrum.[39] This was attributed to overlap of *pi-pi* bonds in the aggregated lignin structure, resulting in bathochromic shift. Similar improvement was observed by Qian et al (2015) who tested reverse micelles against alkali lignin using reflectance spectroscopy.[40] Their reasoning for the improved absorption was due to hydrophobic surface of the particles (yielding the absorbing phenolic groups) however this is not a reasonable assumption as light can easily penetrate through the full diameter of these small particles and be absorbed on the interior. Qian et al (2017) studied the absorption of lignin particles of different sizes in sunscreens. The results demonstrated an increasing improvement in UV protection capabilities with reducing particle diameters from >1000 nm to <100 nm.[41] In summary, the conclusions from studies on the UV absorption activity of lignin particles are inconsistent and further study on this topic is required.

2.2.3 Production

Today, lignin production comes almost entirely as a byproduct of the pulp and paper industry. Close to 50 million tons per year is generated in the form of black liquor, which, from the Kraft process consists of 29-45% lignin and is usually burned as fuel on site.[43,44] The Kraft process uses sodium sulfide and sodium hydroxide solution at elevated temperatures (155-175°C) to remove as much lignin as is viable without degrading the pulp severely (~90%).[27,33] This black liquor contains an organic/inorganic mixture from which lignin can be purified by fractionation, precipitation and acid neutralization.[27]

2.2.4 Lignin Applications

Due to such large variation in processing capabilities and properties of different lignins, the applications in which they can be used also varies on the type and even source of lignin. Currently,

the major use of lignin is an energy source at the pulp mills, while low grade lignins have been used in some applications as a filler such as in cement and composites.[45] For higher value applications however, some modification or processing of the lignin is required. Many of these applications of lignin have been demonstrated, but industrially viable processes have not been established. Some examples of high potential lignin applications are carbon fibres, activated carbon, aromatic chemicals such as phenol and vanillin, and biofuels.[46] The strong UV absorption of lignin and antioxidant properties have also triggered exploration into its use in sunscreens and other protective coatings or films.[47-49] Recently, lignin has been shown to form spherical nanoparticles in aqueous media through a robust and scalable process.[6] This has triggered interest and exploration into the potential applications of these particles which have some unique characteristics and abilities in comparison to unmodified lignin.

2.3 Lignin Colloidal Particles

2.3.1 Introduction

Nanomaterials have been a massive area of research in recent decades and will continue to be as they have many applications and demonstrate interesting phenomena. Although there are products on the market today such as sunscreen with ZnO nanoparticles and socks with Ag nanoparticles, there are still a lot of unknowns about how these materials will affect humans and the environment. Studies are beginning to show that these materials can be quite hazardous if handled incorrectly.[1,3] A tactic for averting these hazards while still capturing the interesting phenomena of nano-scale materials is to utilize biomaterials. While biomaterials at the nano-scale are not guaranteed to be hazard-free, they are at least more easily broken down in both the human body and the environment. Cellulose, the most abundant natural polymer on Earth, has been extensively studied as a nanomaterial.[50] The second most abundant biopolymer, lignin, has until recently found very little value-added application either in bulk or nano-sized form.

2.3.2 Formation

Nano-sized lignin particles have only been recently prepared using a variety of different methods including anti-solvent precipitation, pH change, sonication, and supercritical anti-solvent process. The lignins used, and the results of particle formation are shown in Table 4. It is important to

note that the terminology regarding these lignin particles can be misleading. In the table, the morphology as described by the authors is listed. Almost all authors refer to the lignin particles as 'nano', however the recorded sizes of the particles do not match this description. By definition a nano-material is one in which at least 1 dimension is in the range 1-100 nm. For the purpose of this work, these particle suspensions of lignin will be referred to as colloidal lignin particles (CLPs).

Several methods have been demonstrated to produce CLPs, the most common of which is anti-solvent (nano)precipitation. This method has been demonstrated to work with several solvent systems and often includes a significant pH change. In this method, lignin is first dissolved in a good solvent which for Kraft lignin can include highly alkaline water, THF, ethylene glycol or acetone. The solubility of Kraft lignin from different sources can even vary, as noted by Lievonen et al.[6] Once the lignin is dissolved, it is mixed with an anti-solvent, which causes the lignin polymers to agglomerate into solid structures. Working systems have been established with several different lignins and a few solvent/anti-solvent combinations. In several of the methods acid is used as the anti-solvent, exploiting the pH sensitivity of lignin's solubility.[51-54] The method parameters influencing size that have been reported to include solvent/anti-solvent ratio,[40,53,55] acid concentration,[51-53] lignin concentration,[6,38,53] and speed of mixing.[53] Another common method that has been used is ultrasonication. This method in general has been used to produce capsules rather than solid particles, and the size ranges are much larger than in anti-solvent (nano)precipitation.

One important topic of discussion related to these colloidal particles is the nomenclature associated with their formation. The process can be described as aggregation, precipitation and/or self-assembly, however the common associations with these phenomena can lead to misconceptions with respect to CLPs. Aggregation is defined as "several things grouped together or considered as a whole. Or, the act of gathering something together".[56] Precipitation is "the process of forming a solid, called a chemical precipitate, within a liquid medium".[56] While the formation of CLPs fits both of these definitions, they are often associated with uncontrolled processes that result in large particles. Molecular self-assembly describes a process though which molecular units form structures containing varying degrees of order without external control.[57]

Table 4 *Review summary of lignin colloid, nanoparticle & nanocapsule research*

Reference	Materials	Morphology	Methods	Results
Lignin Particles				
Frangville (2012)	• Low sulfonated lignin	• Nanoparticles	• Lignin dissolved in ethylene glycol; slow addition of HCl • Lignin dissolved in water at high temp; slow addition of NaOH	• First method stable from pH 1-9 • Second method stable below pH 5 • Size dependence on lignin and HCl concentrations and rate of mixing
Lu (2012)	• Organosolv lignin	• Nanoscale	• Supercritical anti-solvent process	• Mean particle size of 144 nm
Jiang (2013)	• Sulfate lignin	• Nano-lignin	• Lignin dissolved in alkaline water (pH = 12); slow addition to PDADMAC solution in water (pH = 12)	• Stable from pH 2-12 at mass ratio of 0.5 • Size and zeta dependence on mass ratio
Qian (2014)	• Alkali lignin from wheat	• Colloidal spheres	• Lignin acetylated; dissolved in THF; water gradually added	• Uniform colloids formed with hydrophobic and hyrdrophilic fractions on interior and exterior respectively
Nair (2014)	• Kraft lignin	• Nanolignin	• Lignin suspended in water; homogenized	• Particles with diameters between 10 and 50 achieved with 4 hours homgoenization
Gilca (2015)	• Wheat straw lignin • Sarkanda grass lignin	• Supracolloids	• Water dispersion; sonicated	• Particle sizes between 10 and 100 nm
Gupta (2015)	• Wheat straw lignin	• Nanoparticles	• Lignin dissolved in ethylene glycol; slow addition of HCl	• Particle sizes between 0.1 and 1 μm • Average particle size 0.181 μm
Nypelo (2015)	• Kraft lignin (low ash)	• Nanoparticles	• Lignin dissolved in aqueous NaOH; added to octane surfactant mixture • Crosslinked with epichlorohydrin	• Particles controlled using surfactant concentration and cross-linking • Particles with diameters between 0.09 and 1 μm
Qian (2015)	• Alkali lignin	• Reverse micelles	• Lignin dissolved in dioxane; cyclohexane gradually added	• Nearly monodisperse suspension obtained with average diameter 240 nm
Richter (2015)	• Kraft lignin	• Lignin-core nanoparticles	• Lignin dissolved in ethylene glycol; rapid addition of HNO_3	• Particle hydrodynamic diameter a function of HNO_3 molarity • Average hydrodynamic diameter 84 ± 5 nm
Lievonen (2016)	• Kraft lignin	• Nanoparticles	• Lignin dissolved in THF; dialysis with deionized water	• Average diameters 200-500 nm • Stable from pH 4-10 • Modifiable with adsorbed electrolytes

Richter (2016)	• Kraft lignin (AT) • Organosolv lignin (HPL)	• Nanoparticles	• Lignin dissolved in ethylene glycol; rapid addition of HNO_3 • Lignin dissolved in acetone; water added	• HPL electrostatically stabilized, AT more complicated interactions (hydration, steric) • Both stable over wide range pH (mild acid to beyond) • AT amphiphilic, HPL highly hydrophobic
Yearla (2016)	• Softwood alkali lignin • Hardwood dioxane lignin	• Nanoparticles	• Lignin dissolved in acetone:water (9:1); Injected rapidly into water	• Average diameters 80 – 104 nm with size distributions 27 – 60 nm • Average diameters increase after 30 days to 86 – 116 nm
Qian (2017)	• Enzymatic hydrolysis lignin • Organosolv lignin	• Colloidal spheres • Nanoparticles	• Lignin dissolved in acetone:water (8:1); mixed with excess water	• Large, medium and small particles prepared using different variations of solution concentrations and added NaCl • Distributions of 20-100, 100-300 & 800-1500 nm
Lignin Capsules				
Tortora (2014)	• Kraft lignin	• Microcapsules	• Lignin dissolved in alkaline water (pH = 9.2); ultrasonicated	• Lignin microcapsules created using ultrasonication
Yiamsawas (2014)	• Lignin	• Nanocontainers	• Lignin dispersed in water with NaCl; mixed with cyclohexane and surfactant	• Lignin nanocontainers with aqueous interior synthesized using selective polyaddition • Particles stable over months and can be biodegraded by laccase
Chen (2016)	• Allyl-functionalized ligninnosulfate	• Nanocapsules	• Lignin dissolved in water; mixed with oil phase; sonicated	• Particle size can be controlled with surfactant and stabilizers • Particle sizes 100-400 nm
Bartzoka (2016)	• Low sulfonated Kraft lignin	• Nanocapsules	• Lignin dissolved in water; mixed with oil phase; sonicated	• Sonication parameters strongly affect size • Particle sizes 0.4-6 μm • Polydispersity 0.2-0.6
Li (2016)	• Kraft lignin	• Nanospheres	• Lignin dissolved in dioxane; water added dropwise	• Average hydrodynamic radius of 145.5 • Observed as thick-shelled hollow spheres

This could also be used to describe the assembly of CLPs, depending on the interpretation of order.

As discussed by Whitesides & Grzybowski (2002), the term self-assembly has been 'overused' due to its somewhat broadly encapsulating definition.[57] At the molecular level the structural nature of lignin creates a lack of consistent pattern within and between colloidal particles. At the scale of the particles themselves however, the surface charge and spherical shape have consistency enough to make an argument for use of the term self-assembled structures. Both precipitation[42,51-54,58-60] and self-assembly[38-41,55] have been used in the work summarized in Table 4, with no dependence on the method of preparation. For the purpose of this work, (nano)precipitation is used to describe the formation of CLPs as done by Yearly and Padmasree (2016).[42]

The complex chemical and physical structure of lignin gives it unique behavioral traits. One example is seen when dissolving lignin in THF. Although it can be fully solubilized over time in pure THF, the solvation is much quicker when a small amount of water is added. This can be attributed to interaction of the water with hydrophilic groups, breaking hydrogen bonds and causing the swelling of the polymer.[36] This increases surface area and makes solvation quicker. The formation of lignin particles by anti-solvent precipitation depends on this amphiphilic behavior to create a spherical surface between two phases. Qian et al (2014) demonstrated this by creating particles with hydrophilic shells in water, and then particles with hydrophobic shells in cyclohexane.[40,55] The schematics and images related to the formation process are shown in Figures 4 and 5. The one significant difference is that if too much cyclohexane is added, the particles aggregate due to lack of repulsion. When the particles have a charged shell as in the system from Figure 5, they can remain stable as a suspension in water and the hydrophobic media can be removed. This makes the charged surface particles easier to work with than un-charged particles, as the latter requires a delicate balance of media contents to maintain dispersion while the former are self-stabilized.

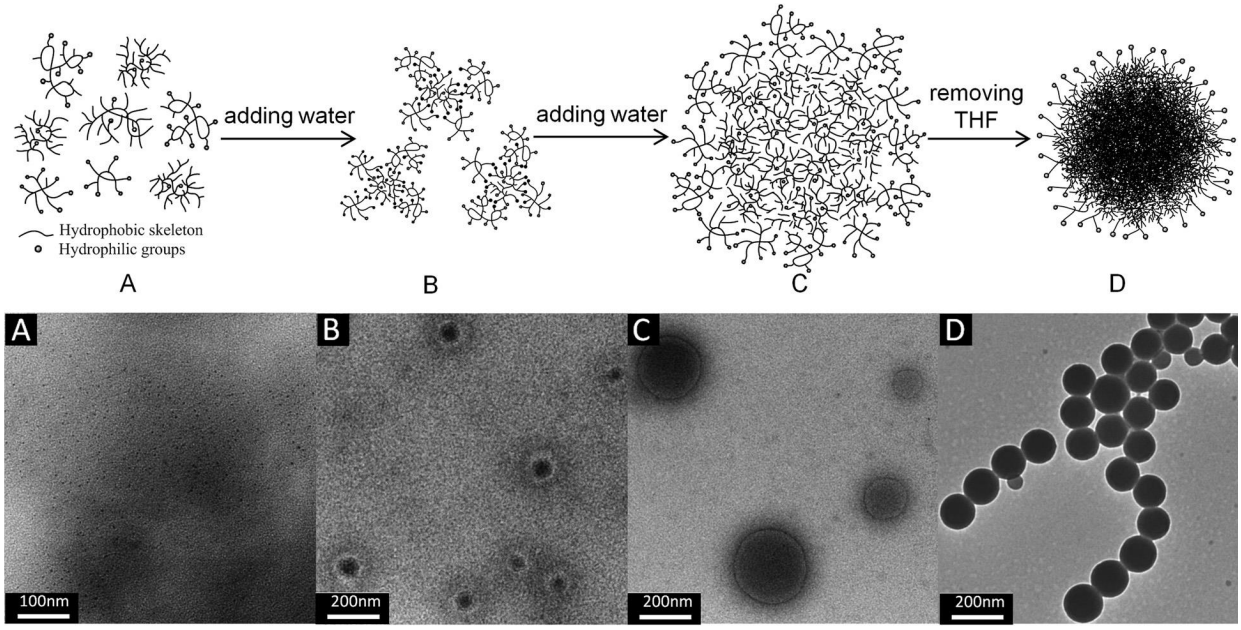

Figure 5 *Self-assembly mechanism during anti-solvent precipitation, water added to THF solution. Adapted from Qian et al (2014)*[55]

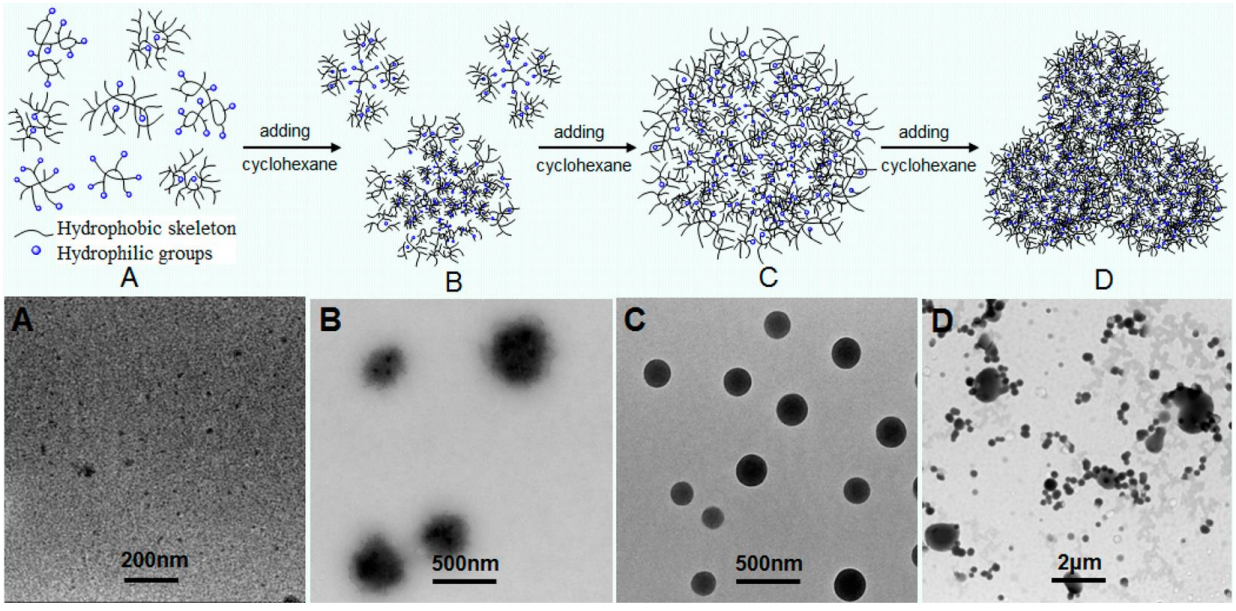

Figure 4 *Self-assembly mechanism during anti-solvent precipitation, cyclohexane added to dioxane solution. Adapted from Qian et al (2015)*[40]

2.3.3 Morphology

The degree of characterization of CLPs has been related to the nature of the work, as some have focused on the particle formation and properties, while others focused on some specific application. The size of CLPs has been recorded in most studies and for the anti-solvent precipitation method the average size is usually 100 – 300 nm with ranges within 50 – 1000 nm.[6,40,42,51-55] Several studies also characterized the morphologies of the particles, which can be spherical as seen in Figure 6.

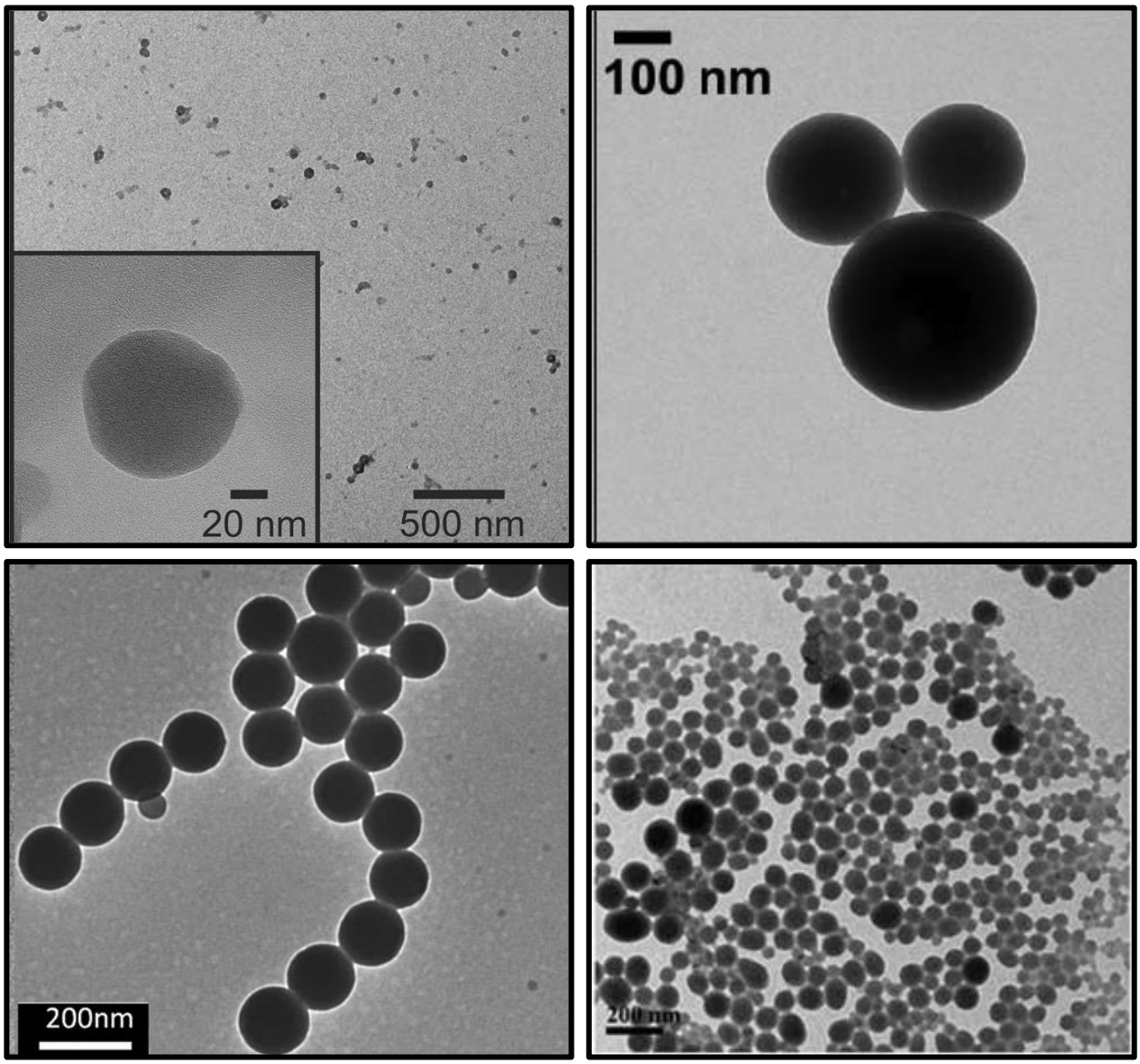

Figure 6 *TEM images of lignin particles formed with different media combinations using the anti-solvent precipitation method. Images adapted from Richter et al (2016)[52] top left, Lievonen et al (2016)[6] top right, Qian et al (2014)[55] bottom left, and Yearla & Padmasree (2016)[42] bottom right*

2.3.4 Colloidal Stability

Colloidal particles are those which are small in size and suspended in a medium of the same or different phase. In the case of CLPs, the solid particles are suspended in a liquid medium.[61] The stability of charged particles can be described by DLVO theory which describes the balance of competing electrostatic repulsion and van der Waals attraction. When colloidal particles are charged, the electrostatic repulsion from like charges on their surfaces pushes them away from each other, preventing flocculation or aggregation.[61,62] If these forces are of sufficient strength, they can maintain stable suspensions of particles by preventing the close proximity interactions where attractive forces begin to dominate. These repulsive forces can be shielded by changing a number of different properties of the suspension such as pH, electrolyte concentration, and surface-active species that adsorb to the colloid surface.[63,64]

When a charged colloid is in an electrolyte solution, the surface charge is balanced by oppositely charged counter-ions that form a layer called the Stern layer. For a negatively charged colloid this stern layer consists of positive ions, which then repel other positive ions at a farther distance also feeling some attraction to the colloid. This balance of attraction and repulsion around the colloid and Stern layer creates a decreasing concentration gradient of positive ions from the edge of the stern layer.[61,63,64] This region is called the diffuse layer which also contains an increasing concentration of negative ions with greater distance from the colloid stern layer. This diffuse layer decreases in charge density as the distance from the colloid decreases, as shown in Figure 7. The Stern and diffuse layers together are called the double layer, and this plays a major role in colloidal stability.[61-63]

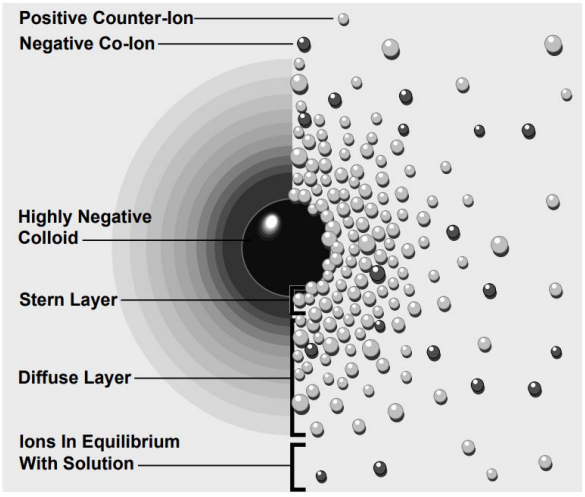

Figure 7 *Diagram of ionic double layer around a charged colloid. Adapted from zeta-meter.com*[63]

The electrical double layer which is formed around charged colloids creates an expanded region of stabilizing repulsion between particles. When particles approach each other, these layers begin to overlap and repel each other. The gradual change of charge density in the double layer creates an electrical potential energy in the

surrounding medium on the order of millivolts.[63] This surface potential can be measured indirectly by tracking the particle movement in an applied voltage field. This electrophoretic mobility can be directly related to zeta potential, which is the potential energy at the boundary between the 'fixed' Stern layer and the surrounding dynamic diffuse layer. This zeta potential can be a valuable tool in measuring the stability of colloidal suspensions by providing information on the electrostatic repulsion that exists between particles.[63,64]

2.4 Scope of Thesis

This work will investigate the formation process of CLPs and their application in wood stains with the main function as UV protection agent. The CLPs are prepared using the solvent/anti-solvent method with THF/water first described by Lievonen et al (2016).[6] Addition methods to mix the two phases are varied along with the rate of addition to test effects on particle size and zeta potential. The prepared particles are then mixed with Tikkurila Oy wood stain, which has had the active UV absorbing ingredient removed. These CLP stains are applied to both Spruce and Siberian Redwood and tested for their weathering resistance compared to the standard wood stain.

3 Experimental

3.1 CLP Preparation

3.1.1 Optimization of Method (Phase 1)

CLPs were prepared using a standard operating procedure developed earlier in this project and based on the work of Lievonen et al (2016).[6] As an initial step for this work (phase 1), the physical mixing parameters of the anti-solvent precipitation method were tested for impacts on CLP formation. First, Lignoboost Kraft (softwood) lignin from Valmet was dissolved in 5:1 mixture of THF:de-ionized water at a concentration of 2 wt%. THF was from VWR chemicals. To form CLPs, the solution was mixed with non-solvent water at a 3:1 vol ratio. For phase 1, several parameters involved in this mixing were tested including type of addition, which

Table 5 *Variations included in CLP formation experiments*

Type of Addition	Rate of Addition	Added Phase
Aerial	Fast	Lignin Solution
Injection	Medium	Water
	Slow	

phase would be stirred and which would be added, and the rate at which the added phase was introduced (Table 5). Aerial addition refers to pouring (fast) or dripping (medium & slow) the added phase to the stirring phase. Injected additions were done with plastic syringes and hypodermic needles depending on the addition rate. Rates of addition were difficult to control as they were done manually with some help from different needle sizes. Time of addition was recorded and the rate was determined as the average of volume divided by time.

3.1.2 Preparation with Optimized Method (Phase 2)

For this phase, the chosen method for CLP preparation was rapid addition of solution phase to stirring water. The lignin solution was prepared in the same way as in phase 1 and added rapidly to stirring de-ionized water. CLP suspensions were stirred for 15 minutes and then dialyzed in de-ionized water for 72 hours using 6-8 kD dialysis tubing from Spectrum Labs. After dialysis, CLPs were filtered through VWR 415 Qualitative filter paper and stored at room temperature.

3.2 Stain Preparation

Wood stains were prepared using the standard wood stain provided by Tikkurila Oy (Finland) with and without standard UV absorbing material. Stains were diluted with water (standard) or CLP suspension by approximately 25 wt%. CLP stains were prepared with weight ratios of 1, 1.5, and 2 relative to the standard UV absorbent.

3.3 Wood Sample Preparation

Spruce heartwood and Siberian Larch were used in this work. Wood samples were initially cut in dimensions of 70 x 150 mm and conditioned at 20°C and 65% humidity. Stain was applied on one surface with a 70 mm synthetic fiber brush until coating was even. Samples were then left to dry in 20°C and 65% humidity for 24 hours before applying a second coat. Samples were conditioned until mass stabilized.

3.4 Artificial Weathering

For UV exposure testing, wood samples were cut to 70 x 44 mm. Two samples of each variation NAT (natural), STD (standard stain) and CLP 1, 1.5, and 2 were tested together. Samples were

placed in the Suntest CPS+ machine from Atlas Material Testing Solutions (United States) operating with a xenon arc lamp. This lamp has emission spectrum very similar to actual sunlight. In unfiltered tests (round 1), radiation wavelengths were in the range 250 – 800 nm. Additional tests were run with a coated glass filter with radiation exposure of 310+ nm (round 2).

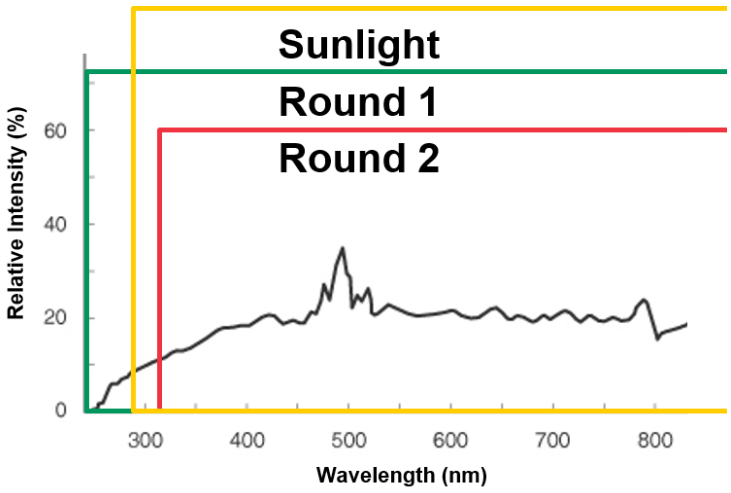

Figure 8 *Irradiance spectrum of Xenon arc lamp (modified from https://www.ushio.co.jp/en/products/1017.html) with filtered limits in round 1& 2 experiments and actual sunlight spectal range.*

These experiments were extremes on either side of actual sunlight exposure as shown in Figure 8, an emission spectrum for xenon arc lamp. Exposure intensity was set at 765 W/m^2 and a black standard temperature of 60°C. Samples were characterized at 0, 0.5, 1, 1.5, 2, 3, 4, 5, 6, 7, 8, 20, 32, 44, 68, and 92 hours of exposure. Characterization included mass and color measurements as well as photographs. As a reference to real weather conditions, sunlight at noon in Florida (United States) has been measured at 15 W/m^2.[49]

One experiment was conducted with unfiltered light and spruce samples where water was added to simulate dew or rain. After 6 hours of total exposure time, 1 ml of de-ionized water was randomly distributed on the sample surfaces after each of the remaining 6 characterization intervals.

3.5 Color Change Analysis

Spectrophotometry was used to characterize wood sample color using a GretagMacbeth (United States) Spectrolino with D65 light. The CIE Lab coordinate system was used and change in color was calculated using Equation 1.

(1) $$\Delta E = \sqrt{\Delta L^2 + \Delta a^2 + \Delta b^2}$$

where: ΔE – color difference,

L – color achromatic coordinate (lightness); L = 100 indicates approximation of a given color to white, and L = 0 to black,

a, b – color chromatic coordinates; (+ a) indicates red color, (– a) indicates green color, (+ b) indicates yellow color, (– b) indicates blue color.

3.6 UV-Vis Spectroscopy

3.6.1 Transmission

UV-vis transmission spectroscopy was carried out using Lambda 950 spectrometer from Perkin Elmer (United States). Tungsten (visible) and D2 (UV) lamps were used with a slit width and data interval of 2 nm. Quartz microscope slides (25.4 x 25.4 x 1 mm) from Alfa Aesar (United States) were coated with STD and CLP1 stains using 20 mm synthetic bristle brush. The stain density of applied coatings is shown in Table 6.

Table 6 *Quartz glass coated stain densities used for UV transmission spectroscopy.*

Sample	**Stain Density (mg/m^2)**
STD	6.24
CLP 1	6.56

3.6.2 Reflection

UV-vis reflection spectroscopy was carried out using a Perkin Elmer (United States) Lambda 950 spectrometer. Tungsten (visible) and D2 (UV) lamps were used with a slit width and data interval of 2 nm.

3.7 Zeta Potential & Particle Size

The zeta potential and particle size of CLPs were analyzed using Zetasizer Nano-ZS90 from Malvern Instruments (United Kingdom). Zeta potential was calculated automatically from measured electrophoretic mobility with the dip-cell probe and using Smoluchowski model. Zeta measurements were conducted at an approximate concentration of 0.9 mg/ml. Size measurements were measured with dynamic light scattering at a concentration of 0.2 mg/ml.

3.8 Contact Angle

Contact angles were measured with KSV Instruments CAM 200 optical contact angle meter. Water droplets of 60 µl were applied to the surface and measurements were taken every second

for 60 seconds. Initial contact angle was marked after 5 seconds of contact to eliminate dropping effects.

3.9 Water Absorption Test

Water absorption testing was done on samples cut to 20 mm x 30 mm x 70 mm. The 4 edges around the stained surface were coated with Sikaflex 11FC All-in-One commercial polyurethane sealant. The coating was allowed to dry and then samples were weighed. The stained surfaces (30 mm x 70 mm) were then placed face down into room temperature tap water for 94 hours, weighing at intervals of 3, 5, 20, 44, and 94 hours.

4 Results & Discussion

4.1 CLP Stain Stability

Due to the complex recipe of wood coatings, the stability of the stain suspension upon addition of CLPs was not certain. The most immediate and obvious change to the stains was the change of color from creamy white to different shades of brown similar to raw lignin color. Increasing the concentration of CLP created a slightly darker color. This color however, is not how it looks when applied to a surface. The white creamy standard stain goes on as a colorless, transparent coating while the CLP stains maintain some of their color but are also transparent, showing the natural features of the wood beneath.

There was quite a notable decrease in viscosity with increasing CLP concentration. Viscosity is a very complex phenomenon, especially in a suspension with so many components, thus the mechanism of this effect is not clear. It is good to note that the CLPs although affecting the suspension stability in some way and decreasing viscosity, did not cause notable destabilization to the point of aggregation. All the stains required some stirring to properly re-disperse the components before staining, however this is normal with several weeks between use. The viscosity change was significant enough to cause issues when applying the stains, which would be problematic for applications requiring the staining of a vertical surface. An important source of error in this work was the application of the stains, done by hand with a brush. During application, the even spreading of the coating was favored more important than applying

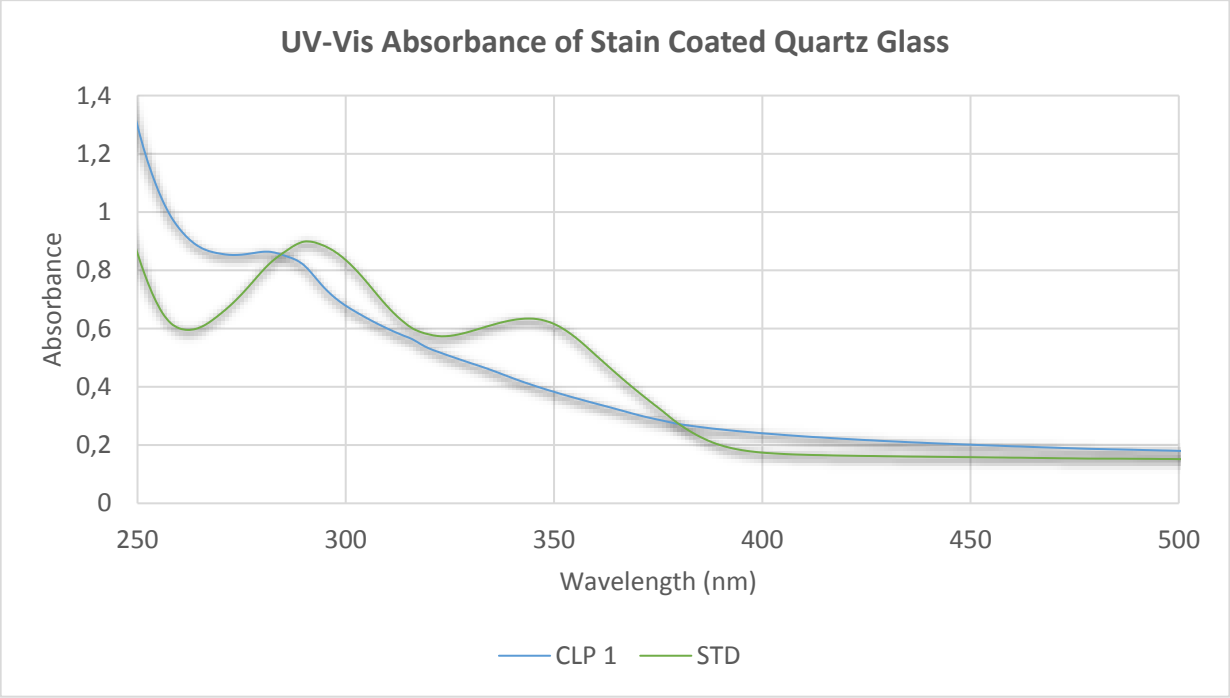

Figure 9 *UV-Vis transmission spectra for CLP 1 and STD coated quartz glass*

identical mass of stain. Consistent application was made difficult by both the small size of wood pieces and the viscosity difference between the 4 stains. This resulted in some variance in coating masses between samples.

The effect of pH on the stain stability (viscosity) was not measured or studied here, however that is a notable parameter that could have significant impact. The pH of CLP suspensions is quite low (3-5) while the operating pH of the stains is about 8. This is an important consideration where stability is concerned and should be studied further. Increasing pH causes a significant increase in the zeta potential of CLPs due to the dissociation of the acidic hydrogens from phenolic and carboxylic groups. This increase in charge at the surface of the particles may cause further destabilization effects in the stains.

4.2 Stain Transmission Spectroscopy

Prior to testing the coatings on wood, the transmission spectra was collected for both CLP 1 and STD stains on quartz glass and is shown in Figure 9. The characteristic absorption peak for lignin at 280 nm is clearly visible, as well as a broad absorption shoulder extending into the visible region. This shoulder is believed to be a combination of scattering effects and bathochromic shift

as discussed by Li et al.[39] Relative to the standard, the CLP coating is notably less absorbent from 330 – 370 nm. Higher absorption in the UVC region (250-290 nm) is irrelevant as this radiation is never reaching the Earth's surface. Higher absorption by lignin in the visible region (400+ nm) may have some benefit (depending greatly on wood species) as shown by the work of Nowaczk-Organista et al (2009).[15] While the absorption capability of lignin is well studied and documented,[30] the purpose of this work was to test the stability of lignin absorption in wood coatings after exposure to weathering effects.

4.3 Suntesting Color Change

4.3.1 Qualitative Observations

Natural and coated samples were exposed to a total of 92 hours of 765 W/m^2 of energy, which can be related to some extent with actual sun exposure. The irradiance at noon in Florida, United States has been recorded at 15 W/m^2. If this irradiance persisted for 8 hours every day for 365 days of the year, the 92 hours of exposure in the suntest machine would be equal to approximately 1.6 years. This is a very conservative estimate, however, because the sun does not shine for 8 hours, 365 days a year, and certainly the Finnish sun exposure is different than in Florida. Additionally, other natural weathering impacts such as temperature fluctuation, moisture, wind and dirt are not experienced by the samples in the suntest and could impact weathering significantly. In any case, regardless of exact natural weathering comparison, the samples of natural wood (NAT), standard stain coated (STD) and three loadings of CLP stains (1, 1.5 & 2) were tested together in each experiment and can be compared on a relative basis.

Photographs of the suntested samples are shown in Figures 10 & 11 for spruce and Siberian larch respectively. Color change has been used as an indicator in many studies on wood photodegradation, as it is an easily measurable and characteristic sign of chemical changes at the surface.[16] In the natural and standard samples, the progression of color change appears somewhat linear in both tone and shade after the initial change at 0.5 hours. The change in color of the standard is notably less intense than the natural sample but still significant after 92 hours. In the spruce samples (Figure 10), the CLP coatings are very noticeably darker in color than the natural and colorless standard coated samples, with shades of red/brown typical of native lignin.

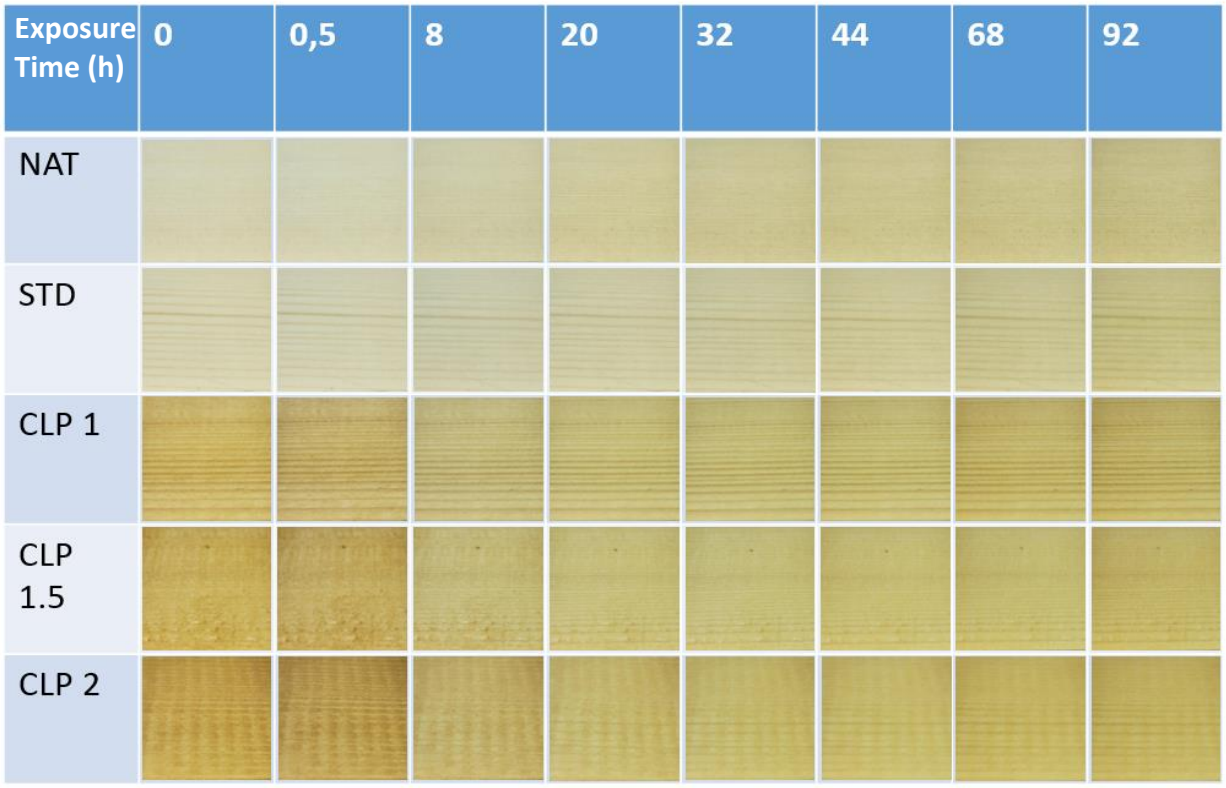

Figure 10 *Photographs of NAT, STD and CLP spruce samples from 0 to 92 hours irradiance in round 2*

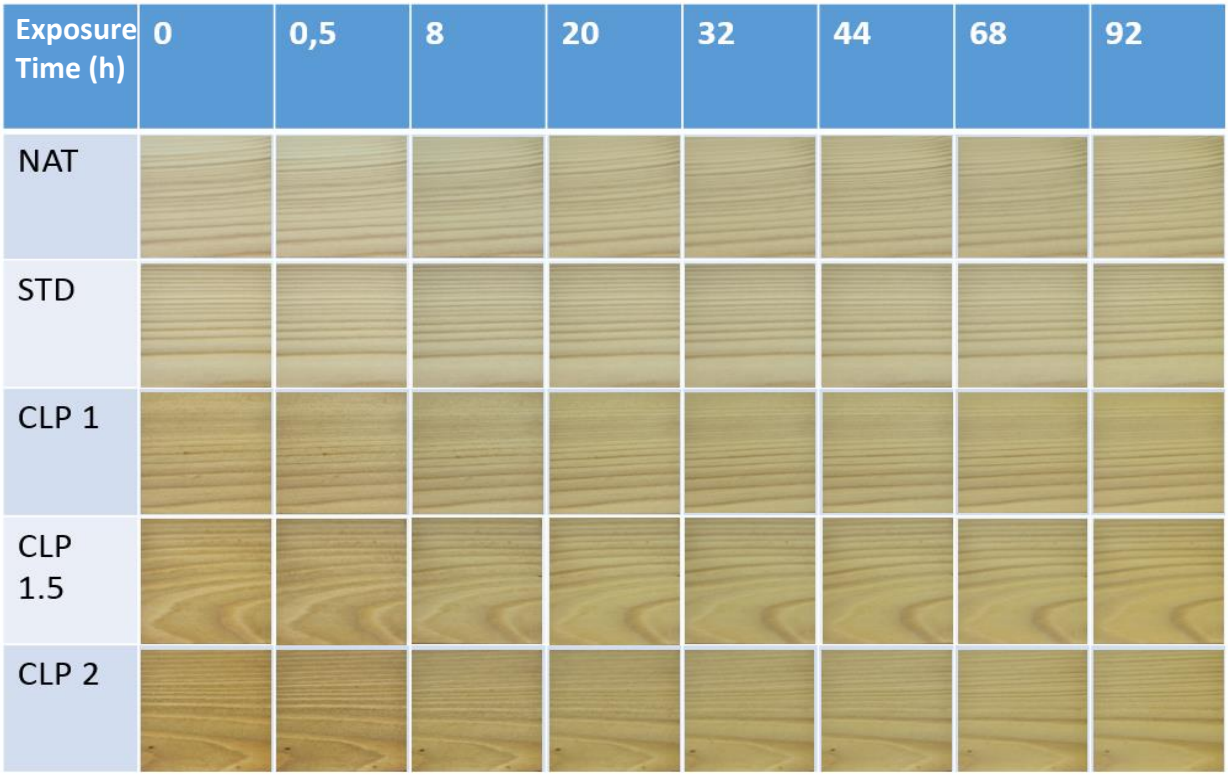

Figure 11 *Photographs of NAT, STD and CLP larch samples from 0 to 92 hours irradiance in round 2*

The difference is much less significant however in the larch samples (Figure 11). This is simply due to the natural dark and reddish color of the larch wood which creates less contrast between the natural wood and CLP coatings. The color change for all samples is also much less significant in the larch samples compared to the spruce, matching the trend of similar change with different magnitudes shown in the work of Oltean et al (2008).[18] For this reason, the spruce samples are easier for qualitatively analyzing the color change progression of the samples. There are interesting trend differences between the CLP samples compared with the NAT and STD samples.

While the progression of color change seems linear in NAT and STD samples, it changes in a more complex fashion for CLP samples. While NAT and STD samples gradually get darker and take on a more grey/yellow shade, the CLP samples go through a more cyclical change. The initial change in CLP samples is more drastic, however they appear after 92 hours of exposure actually closer in color to their original state. The ripples seen in CLP 1.5 and CLP 2 spruce samples are expected to be small ridges from the planing process which are then accentuated by pooling of the dark colored CLPs. The fading of this accentuation is an indication of CLP color loss. Interestingly, a difference in color between CLP 1, 1.5 and 2 in the beginning, but seems to dissipate after longer time of exposure, resulting in similarly colored samples after 92 hours. In fact, the overall color change is greater for CLP 2 samples than CLP 1 samples. This indicates that the overall absorption of the coatings is higher with CLP 2 however it does not indicate the changes underneath the coating. Since the overall color change of CLP 1 is less, it could be that the lower concentration of CLPs is sufficient to protect the wood (within the experimental conditions and timeframe). The fact that the final colors are similar however may indicate that even though the higher CLP concentrations absorb more, they may break down at the same rate. This could be attributed to the close proximity of particles at higher concentrations, allowing for more radical chain reactions to occur. This causes a greater number of broken bonds at higher CLP concentrations for the same number of absorbed photons in the coatings. Another explanation could be however that the CLPs are completely broken down in all samples after 92 hours, and some amount of color change in the wood underneath is occurring. The color of the CLP coatings even after exposure could be effectively masking the change underneath, or the color in the end could be mostly due to the wood showing through the remaining transparent

coating. It was unfortunate in this work that the coatings could not be successfully removed as it would have given much more significance and information to the results and conclusions.

4.3.2 Quantitative Color Change by Photospectrometry

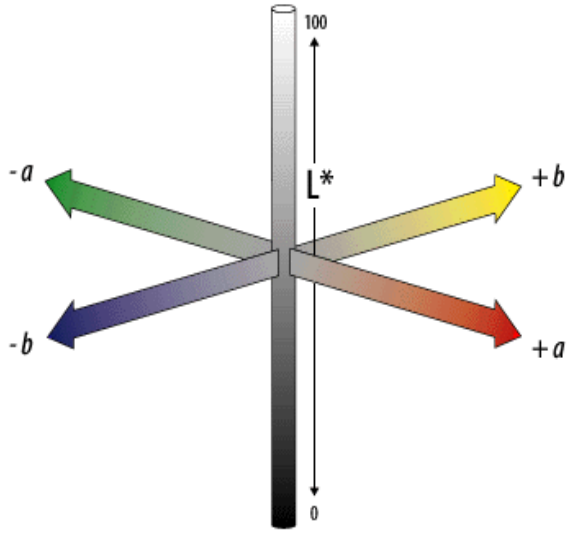

Figure 12 *CIE Lab color coordinates. Taken from http://dba.med.sc.edu/price/irf/Adobe_tg/models/cielab.html*[67]

The color change in the samples discussed qualitatively in the previous section is confirmed here using photospectrometry. In this work, the CIE *Lab* color coordinate system was used to track color changes during suntesting. The color sphere corresponding to the coordinates is shown in Figure 12 to relate the coordinates to axis of color. Spectrophotometer coordinates *Lab* are shown for spruce NAT and CLP 1 samples from round 2 in Figure 13. Although at first glance the graphs appear to be quite different, a closer examination shows that CLP coated samples undergo a very similar change but in a more drawn out fashion. This indicates that a similar mechanism of change may

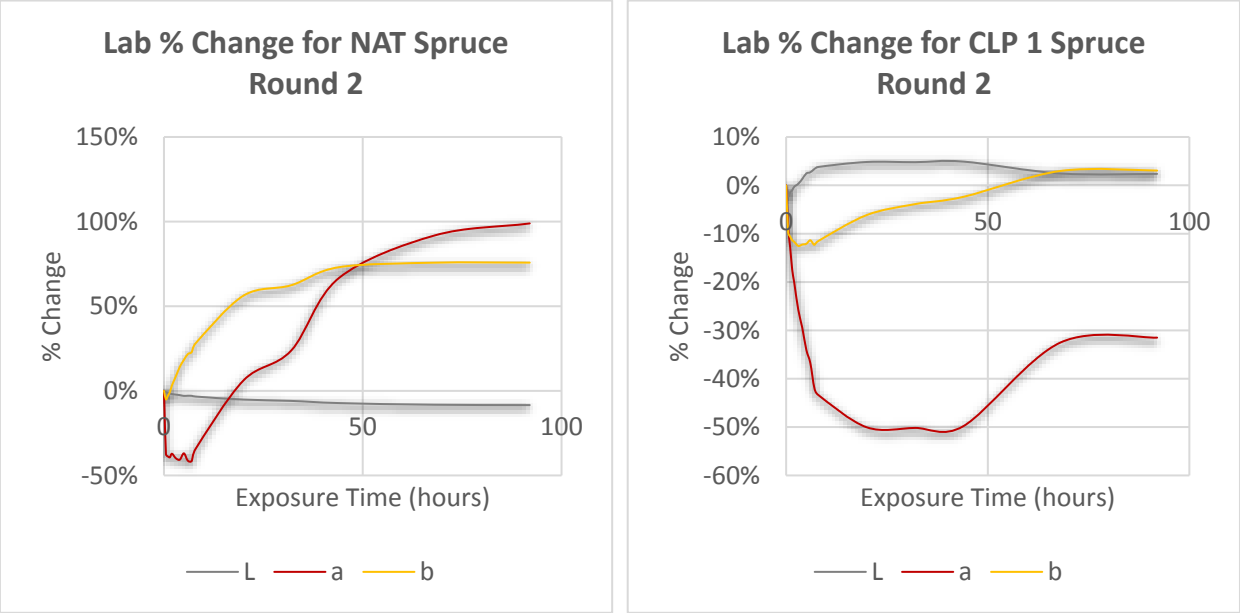

Figure 13 *Color change of L, a, b coordinates for (left) spruce round 2 NAT samples and (right) spruce round 2 CLP 1 samples*

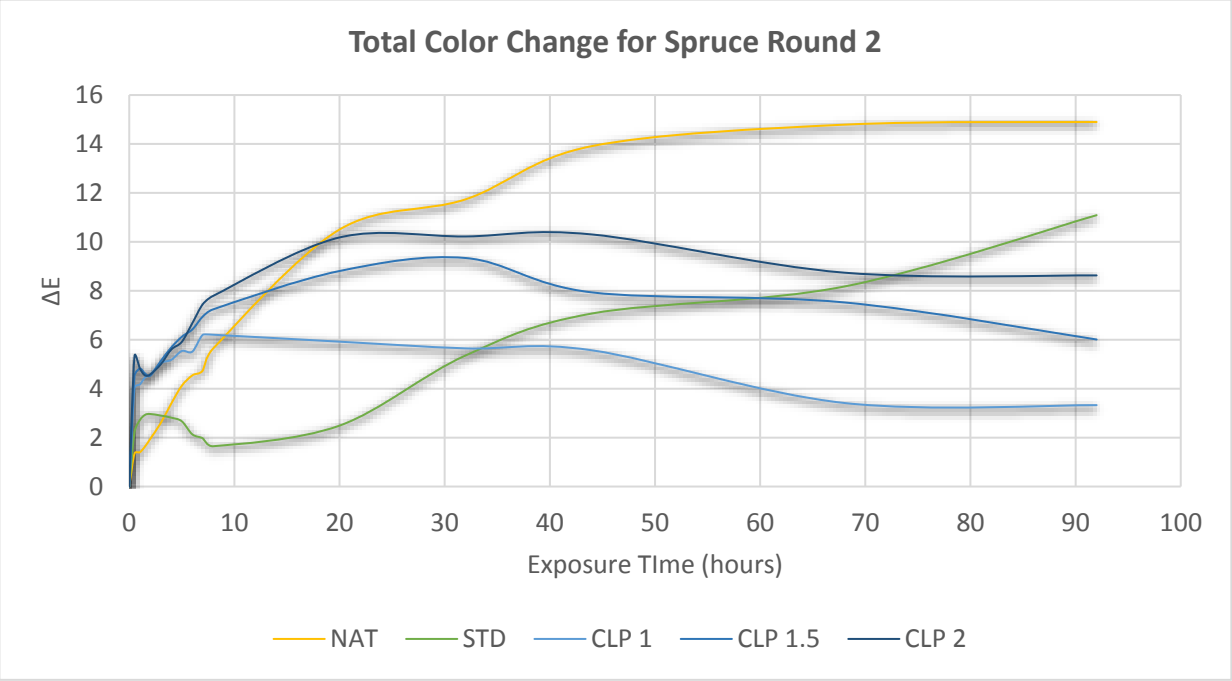

Figure 14 *Total color change for spruce round 2 samples*

be taking place, i.e. the wood underneath the CLP coating changing color. There are however a couple of notable differences. Firstly, aside from the *b* co-ordinate, the natural wood color change continues to increase in magnitude with time. In the CLP coatings however, the color change levels off or at least becomes much less drastic after ca. 70 hours. Additionally, the total color change (max-min) for each co-ordinate is much less intensive (as % change) in the CLP coated samples, and for each axis of color, the color trends toward the original state after different periods of time. The changes observed in the natural samples are consistent with other work such that the wood becomes darker, redder, and yellower over time.[11,15,18,65,66]

The trends are similar when observed as total color change (ΔE) as shown in Figure 14. This is the square root of the summed squares for the 3 co-ordinates, and is shown here as integer value and not as percentage change (representations appear similar regardless). The current representation shows more clearly the differences between CLP coated samples and NAT samples and corresponds more easily with the photographs. The CLPs undergo a much more drastic initial color change but after 92 hours have less magnitudes of total color change to natural and standard coated wood. The effects of CLP concentration can also be clearly seen from the data, with increasing concentration resulting in greater magnitude of color change. These two observations indicate different mechanisms of color change in the coated samples and both

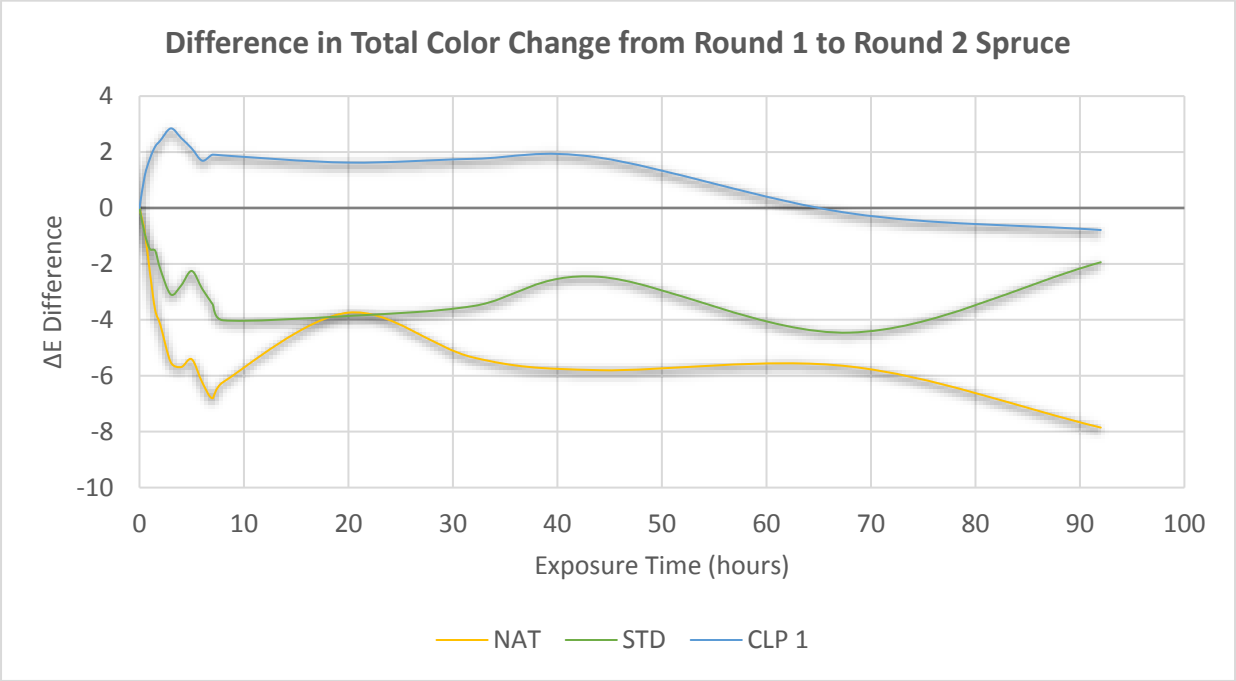

Figure 15 *Total color change difference between round 1 and round 2 spruce samples*

natural and standard coated samples. Since the lignin in wood is the major contributor to color change during UV degradation, the absorbing entities are likely the same, but the overall absorption and progression of degradation is different due to added CLPs. Since the CLPs are somewhat isolated from the wood within the coating, the radicals generated after absorption are unable to affect the wood. This could explain the more drastic initial color change in CLP coatings as the effects remain concentrated at the particles, rather than spreading over the entire surface of the wood. Over long periods of time, this gives the advantage of slower degradation to CLP coated samples as the radical chain reactions are limited due to the isolated particles. In NAT samples, the progression is slower initially due to the larger area of absorbing lignin, however radical formation rapidly escalates the color change due to close proximity of radical sensitive bonds in the wood cells. Qualitatively, the color change observed for natural wood in this study is similar to previously published work.[15,16,18,65,66,68,69]

The focus of discussion has thus far been on round 2 experiments, as they are more realistic in comparison to natural light exposure. Some interesting differences can however be seen when comparing round 1 (250+ nm) and round 2 (310+ nm) spruce color changes in Figure 15. In this figure, negative values in the y axis correspond to a decrease in color change from round 1 to

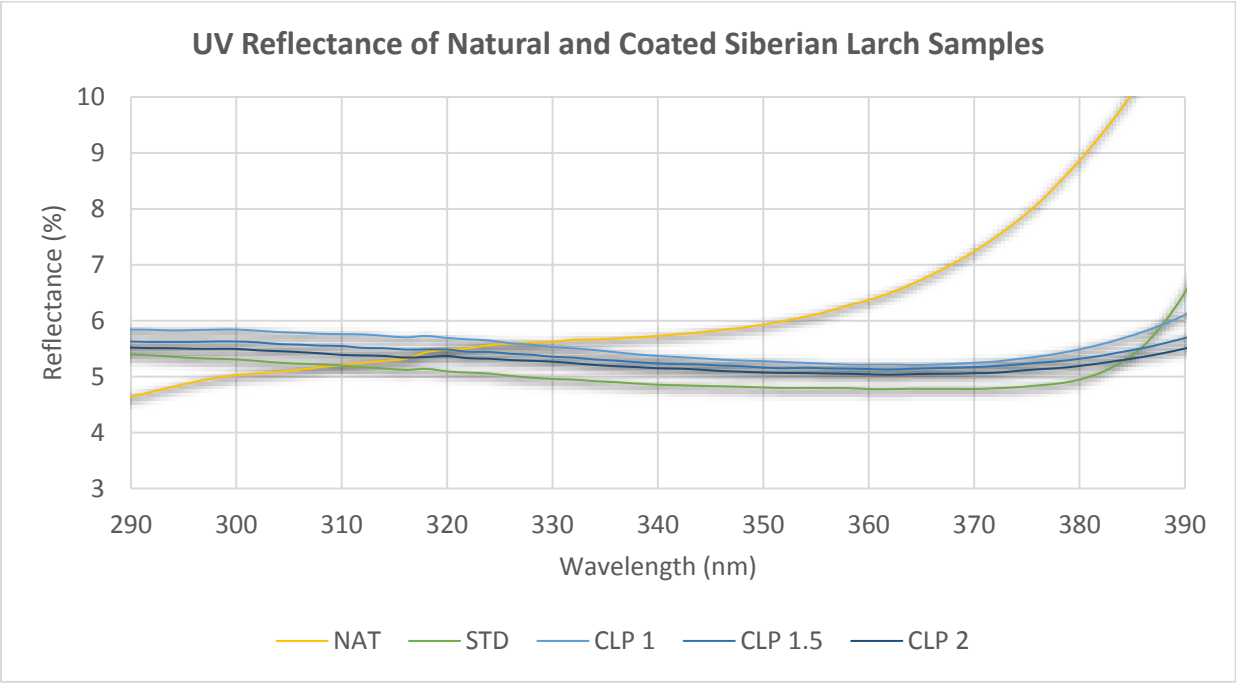

Figure 16 *UV reflectance spectra of unirradiated larch samples*

round 2. It is shown here that the natural sample has an increasingly less change in color with increasing exposure time, indicating that these samples are less affected by lower energy photons (310+ nm) than higher energy (250+ nm). The trend is opposite however, in the CLP coated samples. This increase in color change is due to a re-allocation of power from round 1 to round 2 due to the added filter. The suntest machine compensates for power lost in the spectral region between 250 and 310 nm, which results in amplification of irradiance for wavelengths 310+ nm in round 2. The difference spectra demonstrates that while the NAT and STD samples are more greatly affected by wavelengths less than 310 nm, the opposite is true for the CLP coated samples (at least in first 60 hours). Additionally, the magnitude of the difference indicates good overall stability of the CLP coatings in different irradiance conditions. This is good to note as it is likely the results are quite close to what would occur with an actual sunlight spectrum filter. The opposing trends of CLP and NAT samples indicate different mechanisms by which these samples are changing color. Furthermore, this indicates that in the CLP samples, the observed color change is at least mostly in the coating and not the wood beneath.

4.4 UV-Vis Reflectance Spectroscopy

The differences in color change of wood from round 1 to round 2 shown in Figure 15 can be explained further using UV-vis reflectance spectroscopy. Reflectance spectroscopy allows for the measure of reflected light incident upon solid samples for which transmittance spectroscopy is not possible. Light that is not reflected from the sample surface is assumed to be mostly absorbed by the sample, as transmission in the case here is not possible. Loss of light due to scattering effects is possible, however it is considered to be of little significance relative to the absorbed light. Figure 16 shows the reflectance spectra for Siberian larch samples with no UV exposure. It is shown here that the coated samples are absorbing light between 340 and 390 nm to a greater extent than natural wood. This offers an explanation to why color change increased for coated samples in round 2 while natural samples were more affected in round 1 where they absorb more light below 310 nm.

Aside from the qualitative and quantitative characterization of UV exposure effects, UV reflectance spectroscopy can demonstrate changes in absorption behavior. Figures 17 & 18 show difference spectra for before and after suntesting for round 1 and 2 spruce (Figure 17) and round

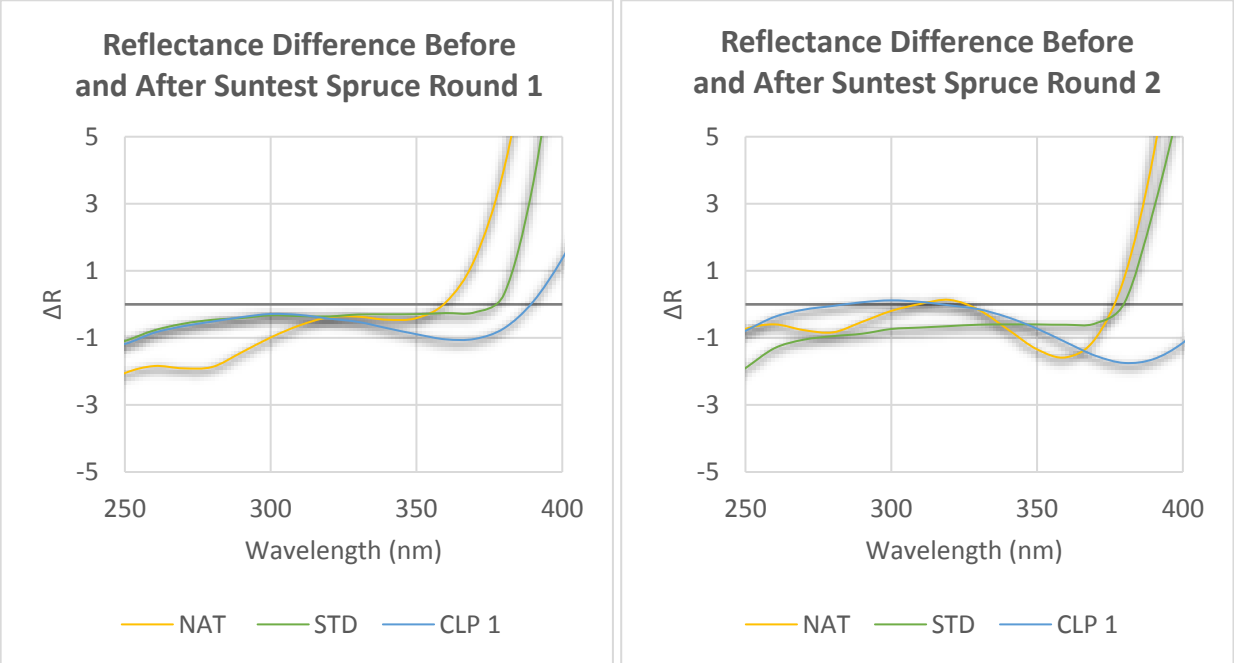

Figure 17 *UV reflectance difference (R1-R2) for (left) round 1 spruce and (right) round 2 spruce samples from unirradiated and irradiated (92h). (+) values correspond to increased absorption after irradiation*

2 larch (Figure 18). In these spectra, a negative ΔR value corresponds to a decrease in absorption after suntesting. Firstly, there is a notable difference between the spruce round 1 and round 2 spectra. Round 1 has more significant absorption decrease at wavelengths below 310 nm. It is important to note that absence of light below 310 nm in round 2 does not mean that components capable of absorbing only higher energy photons will not be degraded. When light is absorbed with sufficient energy, it has a chance to form free radicals. These radicals are in the case of lignin most often a phenoxy radical, stabilized by the aromatic ring. These radicals can delocalize within the aromatic structure, creating a huge variety in degradation pathways and products. This is why the primary lignin absorption peak at 280 nm has also a relatively significant decrease in absorption in round 2 where no light at this wavelength was present.

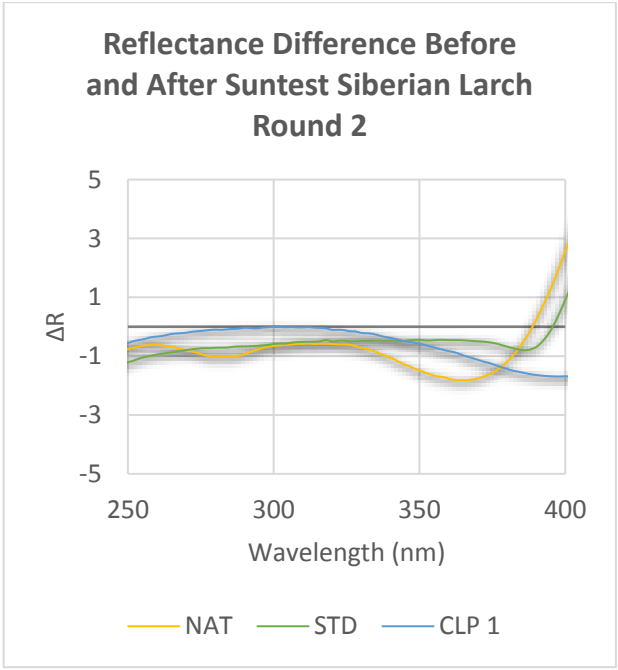

Figure 18 *UV reflectance difference from unirradiated and irradiated (92h) larch round 2 samples (R1-R2). (+) values correspond to increased absorption after irradiation*

A more interesting difference is the large absorption loss in round 2 (both spruce and larch) between 330 and 380 nm which is not seen in round 1 spruce. This could be attributed to the increased irradiance power allocation to these wavelengths as discussed earlier. This suggests direct homolytic cleavage of UV absorbing bonds in that region rather than the progression of more randomized radical initiated degradation seen at 280 nm. Based on the bond dissociation energies shown in Table 2 in section 2.1.2, this peak is likely contributed to mostly by C-C linkages with methyl ether groups attached, absorbing light at 362 nm. A similar decrease in absorption intensity is seen in round 2 for the CLP coated samples, although a red-shifted peak corresponding more to the C-O bond in methyl ether groups (376 nm). Regardless of the reason for this difference between natural and CLP absorption change in round 2, the fact that there is a difference is a promising sign that degradation of the coating rather than of the wood

underneath is occurring. These difference spectra differ from the work done by Pandey & Vuorinen (2008) who found the same increase in reflectance (decreased absorption) at 280 nm after irradiation, but in all higher wavelengths drastic increased absorption.[70] A similar increase in absorption is observed in this work, however not until longer wavelengths of 360+ nm. There could be several reasons for this discrepancy. First, it is important to note that the spectra in the work of Pandey and Vuorinen (2008) are impacted quite dramatically by the lamp change occurring close to 320 nm.[70] This lamp change is a machine-caused error in the mirror alignments in the spectrometer and can cause inaccuracy in the spectra. This may cause some error but the majority of difference is likely due to variations in both experimental conditions and the studied wood species.[70]

There is a very steep increase in absorption that is seen beginning at 360, 380 and 390 nm for NAT, STD and CLP samples in round 1 respectively. This is indicating the generation of chromophores as degradation products. Another promising note here is the large difference between NAT and STD samples and the CLP coated sample which has a much less significant increase in absorption. This may indicate that while there is bond cleavage occurring (seen as negative ΔR), there is some antioxidative property of lignin preventing longer radical chain reactions from occurring. The difference is even more pronounced in round 2. The change in absorption for the STD samples was relatively universal across all wavelengths (between 270 and 370 nm) and rounds. The magnitude of change increased slightly for round 2 samples, indicating as discussed before that the STD color-change mechanism is different as compared to the NAT sample changes. The changes seen here could be a result of the degradation of the UV absorbing component itself. It could also be a result of the coating matrix degradation. Matrix degradation could occur by absorbing photons itself or by reacting with radicals generated within or near the coating. The difference between STD and CLP samples in this region could be demonstrating the antioxidant properties of the CLPs, because the coatings in those samples have not degraded in the same way. Overall, the CLP coatings proved to be more stable in the region of 270 nm to 340 nm (round 2) and 390+ nm but less stable from 340 to 390 nm. It is important to note that these results are for 92 hours exposure in the specific experimental conditions, and that the changes in absorption will differ over time and different exposures.

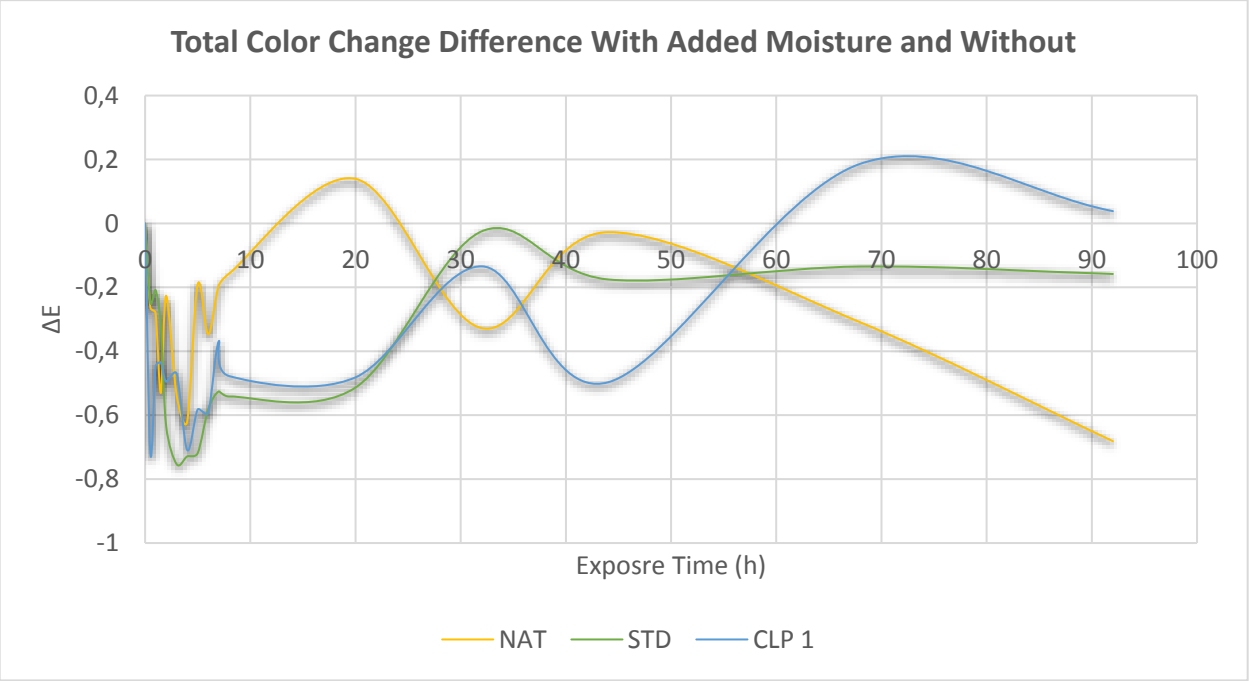

Figure 19 *Color change difference for spruce round 1 samples with and without added water after 6 hours exposure.*

4.5 Water Interaction Effects

4.5.1 Suntesting with Dew Simulation

Moisture can have significant impacts on weathering, mostly by causing stress from swelling and shrinking. The impacts of CLPs in the wood coatings were tested is several ways. The first was to incorporate moisture during suntesting. Figure 19 shows the total color difference for samples with and without added water. In the first 6 hours no moisture was added, so as to act as a reference for error. It can be seen here that there were no significant effects of the moisture in this experiment. This is likely due to the lack of sufficient moisture as only 1 ml was added at each measurement interval. Since the intensity of irradiation is so high, it is likely that this evaporated and was removed from the system before having much interaction with the wood. There does seem to be some increasingly large variation in the NAT and CLP samples however not in any discernable pattern and relative to the difference in the 6 reference hours, it seems insignificant.

Figure 20 *Average contact angles of unirradiated spruce samples*

4.5.2 Contact Angle

One of the main roles of exterior wood coatings is to block large amounts of moisture absorption. Accordingly, in Figure 20 that the coated samples have a significantly higher contact angle than the natural wood. Although only in minor degree, there was a consistently larger contact angle in CLP coatings than the standard. Although this difference of about 5 degrees did not vary between CLP coatings, it could be attributed to CLP surface roughness which affects the contact angle as shown in Equation 2.

(2) $$2\cos\theta^* = \mathrm{r}\cos\theta$$

where $\cos\theta^*$ is the apparent contact angle,

r is the roughness factor $\left(\frac{actual\ surface\ area}{geometric\ surface\ area}\right)$

and $\cos\theta$ is the angle on an ideal surface. This equation was developed by Robert Wenzel and shows how the contact angle increases with increasing surface roughness, while the intrinsic surface energy remains unchanged.[71]

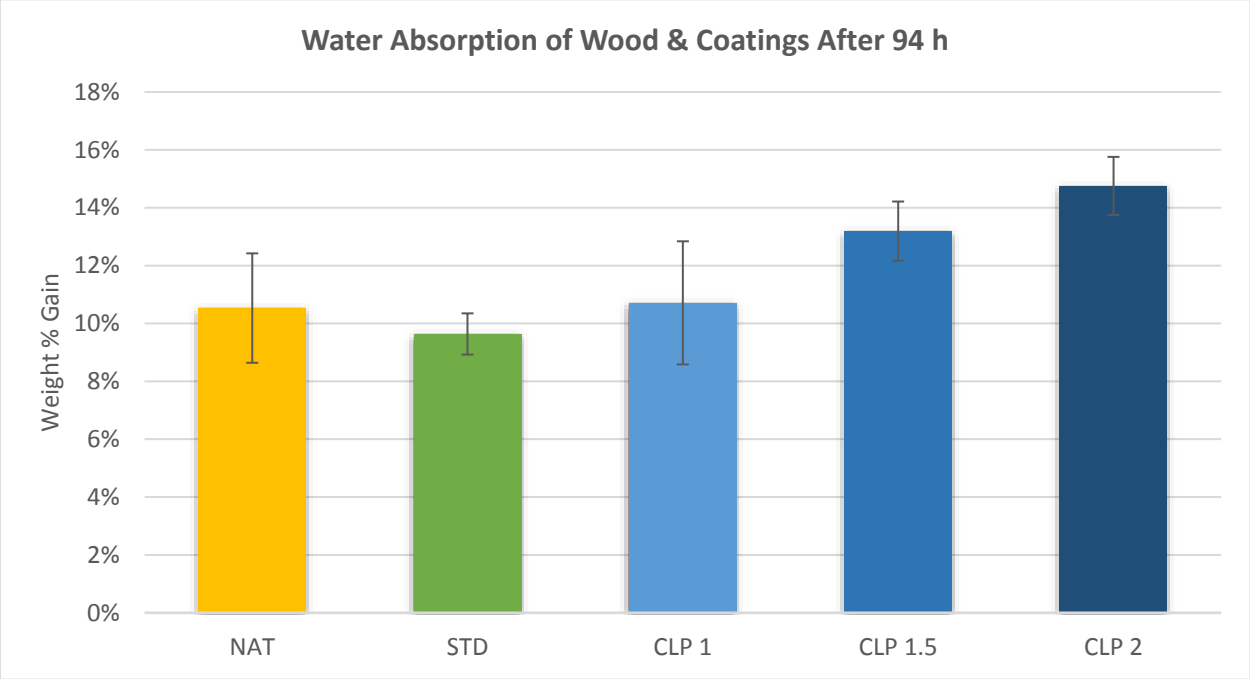

Figure 21 *Water absorption wt% of unirradiated spruce samples*

4.5.3 Water Absorption

While in the contact angle testing it seemed the CLP particles had a small but positive impact on the hydrophobicity of the coatings as compared to the standard coating, the opposite effect was observed in the water absorption test. Figure 21 shows the percentage (weight) of water absorbed by samples after soaking in water for 94 hours. Although variation was large (2 samples for each set), there is a clear trend of increasing absorption with increasing CLP loading in the coatings. Based on the contact angle measurements, it was expected that the coated samples would have similar absorption and would be considerable more resistant than the natural wood. The results show however, that even the standard coating has only a small difference with natural wood when soaked in water for extended period of time. The mechanism by which the CLP facilitate greater absorption is likely the same reason lignin dissolves better in THF with a small amount of added water. Although lignin possesses a significant portion of hydrophobic character, it has functional groups that have quite favorable interactions with water (phenolic and carboxyl). Due to the presence of these groups, lignin can swell to a certain extent with water, which is an important function in the plant cell as well. The lumen of the cell wall is a pathway for water transport through plant cells. The walls of the lumen are composed of lignin which allows the

water to be transported through the cell without being all absorbed by the very hydrophilic cellulosic components. Some absorption is desired however, which the lignin allows, acting as a buffer between the lumen and cell wall.[72] It seems that a similar function takes place in the CLP coatings, in which the lignin could be allowing even greater overall absorption through this swelling behavior. The impacts of surface roughness and surface energy on water interaction with wood coatings was explored by Lozhechnikova et al (2017).[73] It was discovered that although ZnO nanoparticles caused an initial increase in contact angle due to surface roughness, there was a point after increasing concentration that the effect reversed due to the hydrophilic nature. Although lignin itself is not hydrophilic, the nature of the particle formation via fast addition of water causes the hydrophilic parts of lignin to assemble preferentially at the particle surface.[73] This could explain the increased absorption of water with increasing CLP content in this work. The absorption by NAT samples here is similar to the work of Metsä-Kortelainen et al (2006) who conducted a similar experiment with Norway spruce[74] It is worth noting that this experiment included testing of only 2 similarly coated (and natural) samples, which resulted still in great variation. Furthermore, the relative surface area of the coated surface compared to the protected sides was small due to small sample size. This would amplify the effect of any defects in the protective sealant although it is presumed that such small defects would have little impact.

5 Conclusion

This investigation of CLP use for UV absorption in wood stain yielded several interesting and relevant results. Firstly, CLPs were easily mixed into the pre-existing commercial stain. The addition of CLPs with increasing concentration caused a seemingly proportionate decrease in viscosity of the stains, although this was not quantified. The color of both the wet and dry stain was also impacted by addition of CLPs, adding the characteristic brown of lignin to the creamy white (wet) and colorless (dry) standard stain. The extent of the visible color difference in dry films was largely dependent on the wood species. The lighter colored spruce wood showed more drastic color difference between CLP and STD samples compared to the darker Siberian larch.

Prolonged UV exposure resulted in different trends of color change for CLP samples compared with NAT and STD samples. While NAT and STD samples appeared to change in a linear fashion,

CLP samples went through more sporadic color changes. The difference in color progression during UV exposure was confirmed with photospectrometry, which showed that CLP samples actually went through less drastic change relative to their starting color. Additionally, the somewhat cyclical nature of color change in CLP samples resulted in the color after 92 hours being closer to the original color than after 46 hours of exposure. This differed greatly from NAT and STD samples which became increasingly different from their original color with greater time of exposure.

The UV absorption behavior after exposure to UV showed characteristic differences in the spectra absorption behavior. CLP coatings showed highest sensitivity to lower energy absorption bands near the visible region, while showing little change in absorption in the higher energy bands within the sunlight spectrum. STD coatings had a relatively uniform decrease in absorption after 92 hours of exposure in both round 1 and round 2. This decrease was greater than CLP samples for high energy light but smaller for low energy UV light. The absorption behavior of NAT samples after irradiation was more similar to CLP, with large increases over specific regions and little change in others. The exact location of these bands however was different, indicating different absorption behavior or at least mechanisms of degradation. This pattern was consistent in comparing round 1 vs round 2 spruce, as well as round 2 spruce and larch. Small change in the characteristic absorption band at 280 nm for CLP samples indicates good preservation of both CLPs and wood surface.

6 References

1. Aruoja V, Kahru A, Dubourguier H. Toxicity of ZnO, TiO2 and CuO nanoparticles to microalgae pseudokirchneriella subcapitata. *Toxicology Letters*. 2008;180:S220. http://www.sciencedirect.com/science/article/pii/S0378427408009338. doi: 10.1016/j.toxlet.2008.06.088.

2. Auffan M, Wiesner MR, Bottero J, Lowry GV, Jolivet J, Rose J. Towards a definition of inorganic nanoparticles from an environmental, health and safety perspective. *Nature Nanotechnology*. 2009;4(10):634-641. http://dx.doi.org/10.1038/nnano.2009.242. doi: 10.1038/nnano.2009.242.

3. Bondarenko O, Juganson K, Ivask A, Kasemets K, Mortimer M, Kahru A. Toxicity of ag, CuO and ZnO nanoparticles to selected environmentally relevant test organisms and mammalian

cells in vitro: A critical review. *Arch Toxicol*. 2013;87(7):1181-1200. http://www.ncbi.nlm.nih.gov/pubmed/23728526. doi: 10.1007/s00204-013-1079-4.

4. Fajzulin I, Zhu X, Möller M. Nanoparticulate inorganic UV absorbers: A review. *J Coat Technol Res*. 2015;12(4):617-632. doi: 10.1007/s11998-015-9683-2.

5. Hongbo Ma, Phillip L Williams, Stephen A Diamond. Ecotoxicity of manufactured ZnO nanoparticles--a review. *Environmental pollution (Barking, Essex : 1987)*. 2013;172:76-85. http://www.ncbi.nlm.nih.gov/pubmed/22995930. doi: 10.1016/j.envpol.2012.08.011.

6. Lievonen M, Valle-Delgado JJ, Mattinen M, et al. Green chemistry. *Green chemistry*. 2016;18:1416-1422.

7. R. Sam Williams. Weathering of wood. In: Rowell RM, ed. *Handbook of wood chemistry and wood composites, second edition.* CRC Press; 2012.

8. Anderson AB. The composition and structure of wood. *J Chem Educ*. 1958;35(10):487.

9. Weigl M, Pockl J, Muller U, Pretzl H, Grabner M, \. UV-resistance of ammonia treated wood. .

10. Feist WC. Outdoor wood weathering and protection. In: Rowell RM, Barbour JR, eds. *Archaeological wood properties, chemistry, and preservation.* Los Angeles: American Chemical Society; 1988.

11. Teacă C, Roşu D, Bodîrlău R, Roşu L. Structural changes in wood under artificial UV light irradiation determined by FTIR spectroscopy and color. *BioResources*. 2013;8(1):1478-1507.

measurements – A brief review

12. Cogulet A, Blanchet P, Landry V. Wood degradation under UV irradiation: A lignin characterization. *Journal of Photochemistry and Photobiology B: Biology*. 2016;158:184-191.

13. Hon DN, Chang S. Surface degradation of wood by ultraviolet light. *Journal of Polymer Science: Polymer Chemistry Edition*. 1984;22(9):2227-2241.

14. Schaller C, Rogez D. New approaches in wood coating stabilization. *J Coat Technol Res*. 2007;4(4):401-409. doi: 10.1007/s11998-007-9049-5.

15. Nowaczyk-Organista M. Protection of birch and walnut wood colour from the effect of exposure to light using ultra-fine zinc white. *DREWNO-WOOD*. 2009;52.

16. Aloui F, Ahajji A, Irmouli Y, George B, Charrier B, Merlin A. Inorganic UV absorbers for the photostabilisation of wood-clearcoating systems: Comparison with organic UV absorbers. *Applied Surface Science*. 2007;253(8):3737-3745. http://www.sciencedirect.com/science/article/pii/S0169433206011573. doi: 10.1016/j.apsusc.2006.08.029.

17. Browne FL, Simonson HC. The penetration of light into wood. *Forest Prod J*. 1957;7:308-314.

18. Oltean L, Teischinger A, Hansmann C. Wood surface discolouration due to simulated indoor sunlight exposure. *Holz Roh Werkst*. 2008;66(1):51-56. doi: 10.1007/s00107-007-0201-9.

19. Rånby BG, Rabek JF. *Photodegradation, photo-oxidation and photostabilization of polymers.* London: Wiley; 1975.

20. Flexner B. *Understanding wood finishing.* Rodale Press; 1996.

21. Rowell R, Pettersen R, Han J, Rowell J, Tshabalala M. Cell wall chemistry. In: Rowell R, ed. *Handbook of wood chemistry and wood composites.* CRC Press; 2005:43-45.

22. Chakar FS, Ragauskas AJ. Review of current and future softwood kraft lignin process chemistry. *Industrial Crops & Products*. 2004;20(2):131-141. http://www.sciencedirect.com/science/article/pii/S0926669004000664. doi: 10.1016/j.indcrop.2004.04.016.

23. Sjostrom E. *Wood chemistry: Fundamentals and applications.* Second ed. San Diego: Academic Press Inc.; 1993.

24. Brodin I. Chemical properties and thermal behavior of kraft lignins. . 2009.

25. Thakur VK, Thakur MK, Raghavan P, Kessler M. Progress in green polymer composites from lignin for multifunctional applications: A review. *ACS Sustainable Chem. Eng.* 2014(2):1072-1092. doi: 10.1021/sc500087z.

26. Saito T, Perkins JH, Vautard F, et al. Methanol fractionation of softwood kraft lignin: Impact on the lignin properties. *ChemSusChem*. 2014;7(1):221-228. http://www.ncbi.nlm.nih.gov/pubmed/24458739. doi: 10.1002/cssc.201300509.

27. Doherty WOS, Mousavioun P, Fellows CM. Value-adding to cellulosic ethanol: Lignin polymers. *Industrial Crops & Products*. 2011;33(2):259-276. http://www.sciencedirect.com/science/article/pii/S0926669010002670. doi: 10.1016/j.indcrop.2010.10.022.

28. Lora J, Glasser W. Recent industrial applications of lignin: A sustainable alternative to nonrenewable materials. *Journal of Polymers and the Environment*. 2002;10(1):39-48. http://search.proquest.com/docview/758758952. doi: 1021070006895.

29. Evandro Novaes, Matias Kirst, Vincent Chiang, Heike Winter-Sederoff, Ronald Sederoff. Lignin and biomass: A negative correlation for wood formation and lignin content in trees. *Plant Physiology*. 2010;154(2):555. http://search.proquest.com/docview/757815096.

30. Kai D, Tan MJ, Chee PL, Chua YK, Yap YL, Loh XJ. Towards lignin-based functional materials in a sustainable world. *Green Chem*. 2016;18(5):1175-12. doi: 10.1039/c5gc02616d.

31. Varanasi P, Singh P, Auer M, Adams PD, Simmons BA, Singh S. Survey of renewable chemicals produced from lignocellulosic biomass during ionic liquid pretreatment. *Biotechnology for biofuels*. 2013;6(1):14. http://www.ncbi.nlm.nih.gov/pubmed/23356589. doi: 10.1186/1754-6834-6-14.

32. Boerjan W, Ralph J, Baucher M. Lignin biosynthesis. *Annual review of plant biology*. 2003;54(1):519-546. http://www.ncbi.nlm.nih.gov/pubmed/14503002. doi: 10.1146/annurev.arplant.54.031902.134938.

33. Sevastyanova O, Helander M, Chowdhury S, et al. Tailoring the molecular and thermo–mechanical properties of kraft lignin by ultrafiltration. *Journal of Applied Polymer Science*. 2014;131(18):9505-9515. http://onlinelibrary.wiley.com/doi/10.1002/app.40799/abstract. doi: 10.1002/app.40799.

34. Lange H, Rulli F, Crestini C. Gel permeation chromatography in determining molecular weights of lignins: Critical aspects revisited for improved utility in the development of novel materials. *ACS Sustainable Chemistry & Engineering*. 2016;4(10):5167-5180.

35. Hatakeyama T, Hatakeyama H. Lignin structure, properties, and applications. *Adv Polym Sci*. 2010(232):1-63.

36. Hatakeyama T, Hirose S, Hatakeyama H. Differential scanning calorimetric studies on bound water in 1, 4-dioxane acidolysis lignin. *Macromolecular Chemistry and Physics*. 1983;184(6):1265-1274.

37. Mörck R, Reimann A, Kringstad KP. Fractionation of kraft lignin by successive extraction with organic solvents. *Holzforschung*. 1988;48:11-116.

38. Jiang C, He H, Jiang H, Ma L, Jia DM. Nano-lignin filled natural rubber composites: Preparation and characterization. *Express Polymer Letters*. 2013;7(5):480-493. https://doaj.org/article/5407278d692847e89ab0fa221b635e16. doi: 10.3144/expresspolymlett.2013.44.

39. Hao Li, Yonghong Deng, Haisong Wu, et al. Self-assembly of kraft lignin into nanospheres in dioxane-water mixtures. *Holzforschung*. 2016;70(8):725-731. http://www.degruyter.com/doi/10.1515/hf-2015-0238. doi: 10.1515/hf-2015-0238.

40. Qian Y, Qiu X, Zhong X, et al. Lignin reverse micelles for UV-absorbing and high mechanical performance thermoplastics. *Industrial & Engineering Chemistry Research*. 2015:12025-12030. http://catalog.hathitrust.org/Record/001542096.

41. Qian Y, Zhong X, Li Y, Qiu X. Fabrication of uniform lignin colloidal spheres for developing natural broad-spectrum sunscreens with high sun protection factor. *Industrial Crops and Products*. 2017;101:54-60. http://www.sciencedirect.com/science/journal/09266690.

42. Yearla SR, Padmasree K. Preparation and characterisation of lignin nanoparticles: Evaluation of their potential as antioxidants and UV protectants. *Journal of Experimental Nanoscience*. 2016;11(4):289-302. http://www.tandfonline.com/doi/abs/10.1080/17458080.2015.1055842. doi: 10.1080/17458080.2015.1055842.

43. Glasser WG, Kelley SS. *Concise encyclopedia of polymer science and engineering.* Wiley; 1990:544.

44. Alén R, Sjostrom E, Vaskikari P. Carbon dioxide precipitation of lignin from alkaline pulping liquors. *Cellulose chemistry and technology*. 1985.

45. Norgren M, Edlund H. Lignin: Recent advances and emerging applications. *Current Opinion in Colloid & Interface Science*. 2014;19(5):409-416.

46. Smolarski N. High-value opportunities for lignin: Unlocking its potential. . 2012.

47. Sadeghifar H, Venditti R, Jur J, Gorga RE, Pawlak JJ. Cellulose lignin biodegradable and flexible UV protection film. *ACS Sustainable Chem. Eng.* 2017;5:625-631.

48. Peng Y, Liu R, Cao J, Chen Y. Effects of UV weathering on surface properties of polypropylene composites reinforced with wood flour, lignin, and cellulose. *Applied Surface Science*. 2014;317:385-392. doi: 10.1016/j.apsusc.2014.08.140.

49. Jairam S, Bucklin R, Correll M, et al. UV resistance of polystyrene co-butyl acrylate (PSBA) encapsulated lignin–saponite nanohybrid composite film. *Materials & Design*. 2016;90:151-156. doi: 10.1016/j.matdes.2015.10.118.

50. Abitbol T, Rivkin A, Cao Y, et al. Nanocellulose, a tiny fiber with huge applications. *Current Opinion in Biotechnology*. 2016;39:76-88. http://www.sciencedirect.com/science/article/pii/S0958166916000045. doi: //dx.doi.org/10.1016/j.copbio.2016.01.002.

51. Richter A, Brown J, Bharti B, et al. An environmentally benign antimicrobial nanoparticle based on a silver-infused lignin core. *Nature Nanotechnology*. 2015;10(9):817-823. http://www.narcis.nl/publication/RecordID/oai:library.wur.nl:wurpubs%2F489586. doi: 10.1038/nnano.2015.141.

52. Richter AP, Bharti B, Armstrong HB, et al. Synthesis and characterization of biodegradable lignin nanoparticles with tunable surface properties. *Langmuir : the ACS journal of surfaces and colloids*. 2016;32(25):6468. http://www.ncbi.nlm.nih.gov/pubmed/27268077.

53. Frangville C, Rutkevicius M, Richter AP, Velev OD, Stoyanov SD, Paunov VN. Fabrication of environmentally biodegradable lignin nanoparticles. *ChemPhysChem*. 2012;13(18):4235-4243. http://www.narcis.nl/publication/RecordID/oai:library.wur.nl:wurpubs%2F441238. doi: 10.1002/cphc.201200537.

54. Gupta AK, Mohanty S, Nayak SK. Influence of addition of vapor grown carbon fibers on mechanical, thermal and biodegradation properties of lignin nanoparticle filled bio-poly(trimethylene terephthalate) hybrid nanocomposites. *RSC Adv*. 2015;5(69):5628-5636. doi: 10.1039/c5ra07828h.

55. Qian Y, Deng Y, Qiu X, Li H, Yang D. Formation of uniform colloidal spheres from lignin, a renewable resource recovered from pulping spent liquor. *Green chemistry*. 2014;16:2156.

56. The National Academies of Sciences, Engineering, and Medicine. *Transportation research thesaurus.* ; 2017. http://trt.trb.org/trt.asp?NN=Scpb. Accessed June 2017.

57. Whitesides G, Grzybowski B. Self assembly at all scales. *Science*. 2002;295:2418-2421.

58. Lu Q, Zhu M, Zu Y, et al. Comparative antioxidant activity of nanoscale lignin prepared by a supercritical antisolvent (SAS) process with non-nanoscale lignin. *Food Chemistry*. 2012;135(1):63-67. doi: 10.1016/j.foodchem.2012.04.070.

59. Nair SS, Sharma S, Pu Y, et al. High shear homogenization of lignin to nanolignin and thermal stability of Nanolignin-Polyvinyl alcohol blends. *ChemSusChem*. 2014;7(12):3513-3520. http://onlinelibrary.wiley.com/doi/10.1002/cssc.201402314/abstract. doi: 10.1002/cssc.201402314.

60. Nypelö TE, Carrillo CA, Rojas OJ. Lignin supracolloids synthesized from (W/O) microemulsions: Use in the interfacial stabilization of pickering systems and organic carriers for silver metal. *Soft matter*. 2015;11(10):2046-2054. http://www.ncbi.nlm.nih.gov/pubmed/25629687. doi: 10.1039/C4SM02851A.

61. Tadros TF. *Colloid stability: The role of surface forces - part I.* Wiley; 2006. https://books.google.fi/books?id=iLZcSQAACAAJ.

62. Goodwin JW. Interactions between colloidal particles. In: *Colloids and interfaces with surfactants and polymers - an introduction.* John Wiley & Sons, Ltd; 2004:61-93. http://dx.doi.org/10.1002/0470093919.ch3. 10.1002/0470093919.ch3.

63. Zeta-Meter Inc. Zeta potential:. *http://www.zeta-meter.com/*. A complete course in 5 minutes. Accessed June 2017

64. Goodwin JW. The stability of dispersions. In: *Colloids and interfaces with surfactants and polymers - an introduction.* John Wiley & Sons, Ltd; 2004:127-151. http://dx.doi.org/10.1002/0470093919.ch5. 10.1002/0470093919.ch5.

65. Stachowiak-Wencek A, Zborowska M, Waliszewska B, Pradzynski W. FTIR and colour change of pine wood as a result of xenon irradiation. *Forestry and Wood Technology*. 2015;92:425-429.

66. Weichelt F, Emmler R, Flyunt R, Beyer E, Buchmeiser MR, Beyer M. ZnO-based UV nanocomposites for wood coatings in outdoor applications. *Macromolecular Materials and Engineering*. 2010;295:130-136. doi: 10.1002/mame.200900135.

67. Adobe Systems. Color models - CIELAB. . 2000. Accessed June 2017

68. Ayadi N, Lejeune F, Charrier F, Charrier B, Merlin A. Color stability of heat-treated wood during artificial weathering. *Holz Roh Werkst*. 2003;61(3):221-226. doi: 10.1007/s00107-003-0389-2.

69. Custódio JEP, Eusébio MI. Waterborne acrylic varnishes durability on wood surfaces for exterior exposure. *Progress in Organic Coatings*. 2006;56(1):59-67. http://www.sciencedirect.com/science/article/pii/S0300944006000464. doi: 10.1016/j.porgcoat.2006.02.008.

70. Pandey KK, Vuorinen T. Comparative study of photodegradation of wood by a UV laser and a xenon light source. *Polymer Degradation and Stability*. 2008;93(12):2138-2146. http://www.sciencedirect.com/science/article/pii/S0141391008002826. doi: 10.1016/j.polymdegradstab.2008.08.013.

71. Wenzel R. Resistance of solid surfaces to wetting by water. *Industrial and Engineering Chemistry*. 1936;28.

72. Brett CT, Waldron KW. *Physiology and biochemistry of plant cell walls.* Springer Netherlands; 2012. https://books.google.fi/books?id=zEfzCAAAQBAJ.

73. Lozhechnikova A, Bellanger H, Michen B, Burgert I, Österberg M. Surfactant-free carnauba wax dispersion and its use for layer-by-layer assembled protective surface coatings on wood. *Applied Surface Science*. 2017;396:1273-1281. doi: 10.1016/j.apsusc.2016.11.132.

74. Metsä-Kortelainen S, Antikainen T, Viitaniemi P. The water absorption of sapwood and heartwood of scots pine and norway spruce heat-treated at 170 °C, 190 °C, 210 °C and 230 °C. *Holz Roh Werkst*. 2006;64(3):192-197. doi: 10.1007/s00107-005-0063-y.

7 Appendices

7.1 Appendix 1 – CLP Preparation

7.1.1 CLP Preparation Figures

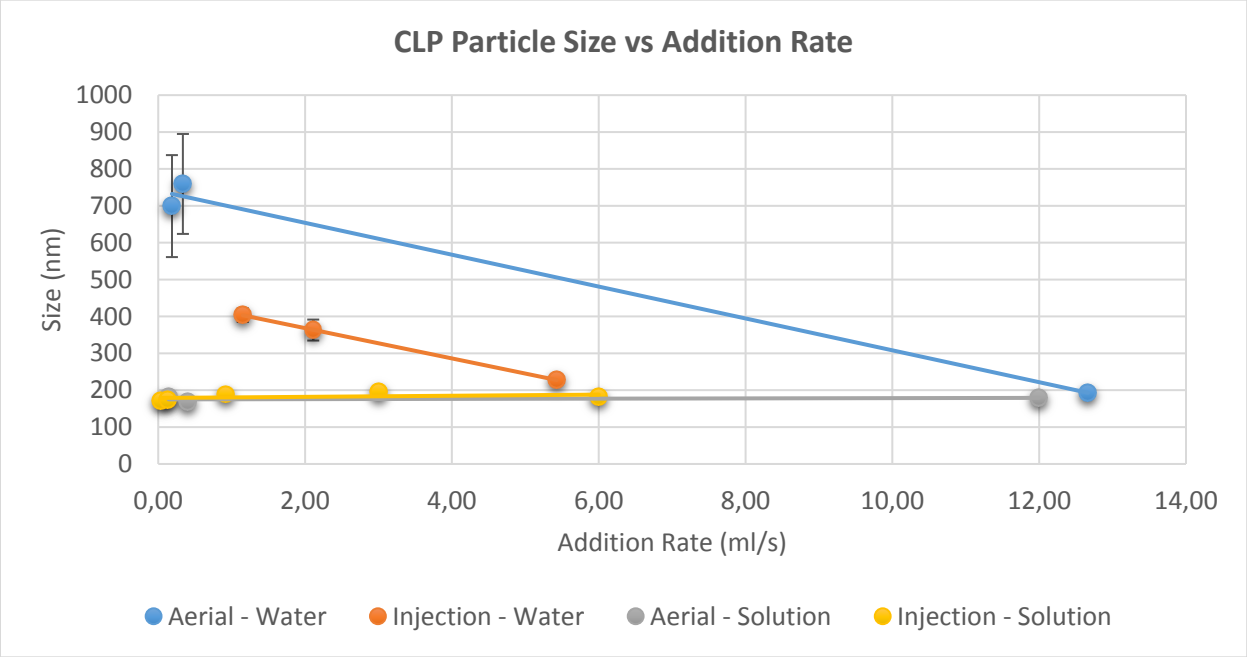

Figure 1 *CLP average particle size vs addition rate of both water and solution phases using aerial and injection methods.*

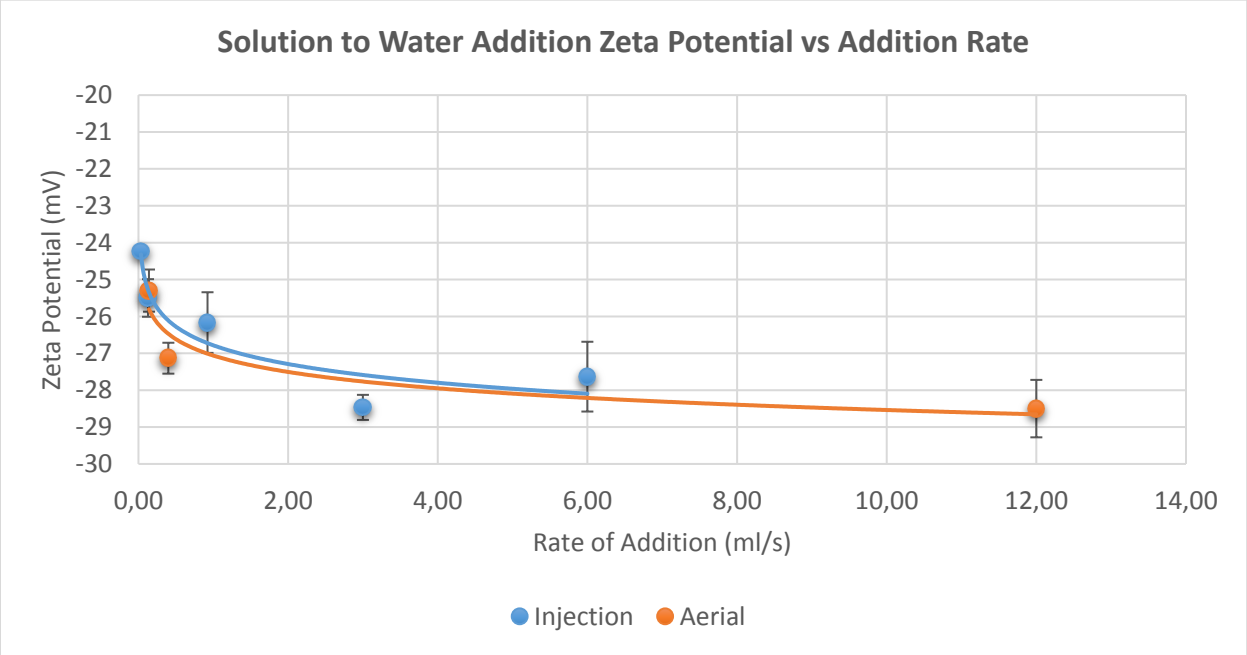

Figure 2 *CLP average zeta potential vs addition rate for solution to water addition using aerial and injection methods.*

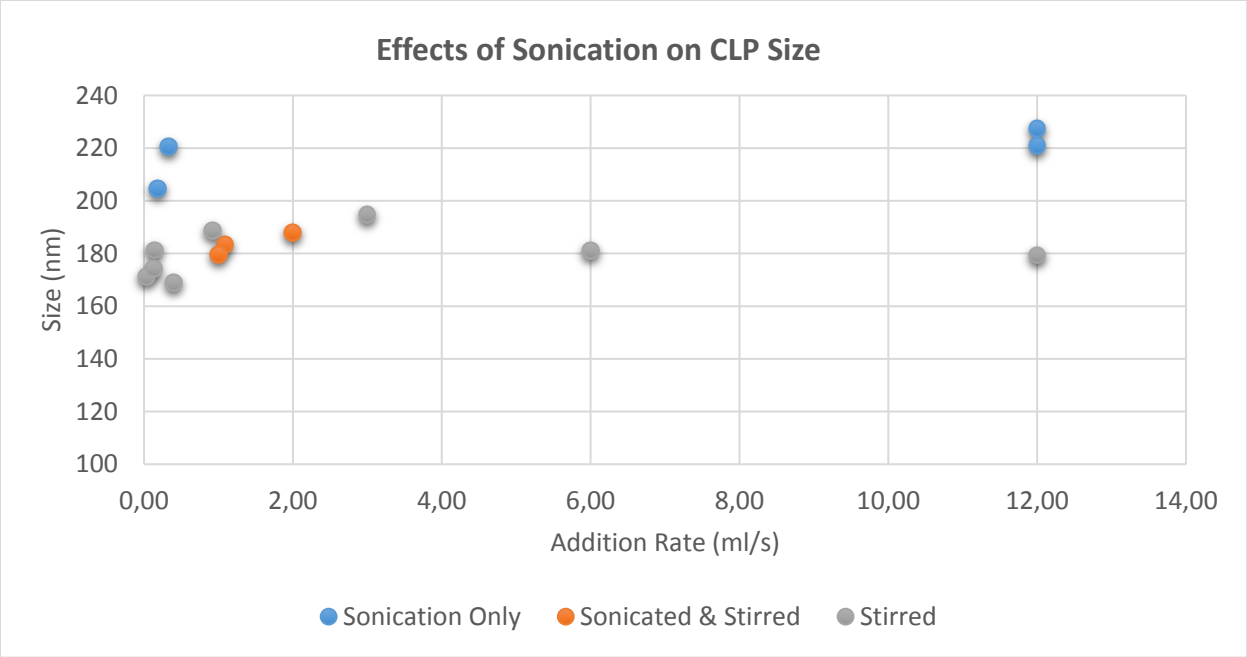

Figure 3 *CLP average particle size vs addition rate for solution to water addition with stirring, sonication only, and sonication with stirring*

7.1.2 Discussion of CLP Preparation Experiments

The mechanisms of particle formation are complex and some factors contributing to their final size and zeta potential were explored in this work. The purpose of these experiments was to examine the physical modes of control that affect formation. Since the particles are formed during the mixing of the lignin solution and the anti-solvent water phase, some variations in how these phases are combined were explored. This included which phase would be added to the other, the method of addition, and the stirring or sonication effects during addition.

One important result of these experiments was that the rate of addition can have significant impact on particle formation, when water is being added to solution (Figure 1). When the solution is added to stirring water however, the rate of addition becomes irrelevant. The reason for this is that in order for stable particles to form, a certain concentration of anti-solvent is required at the time of formation. When water is added slowly, the low concentration begins to cause precipitation of the lignin but is not high enough to cause spherical particle formation. The result is much larger agglomerates that aggregate quickly after mixing. When the solution is added to water however, the concentration of water is always high enough to cause particle formation, so the speed of addition does not have an effect.

The effects of addition rate on zeta potential for solution to water addition only are shown in Figure 2. There seems to be a correlation between increasing addition rate and increasing magnitude of zeta potential, however more data is needed before making that conclusion. The cause of this relationship is a little more difficult to explain. It could be that adding the solution slowly allows the particles to reach a more preferential organization, while adding rapidly causes a more spontaneous arrangement. This means that polar groups such as hydroxyls and carboxyls arrange on the surface of the particles, giving them a higher negative zeta potential.

Lastly, the effects of the stirring and sonication during addition were examined. Figure 3 shows the rate of addition relationship with sonication only, stirring only, and then sonication with stirring. The addition rate alone did not appear to have any effects, and neither did sonication as long as there was stirring. Without stirring however, sonication caused slightly larger particles to form. It was hypothesized that the sonication might help create smaller particles by reducing aggregation but it is possible the opposite occurred.